



Air Force Academy

# **Development of a F.W.M.A.V. with livestreaming capabilities**

**Gonçalo dos Santos Raminhos**

*Aspirante a Oficial-Aluno/Piloto-Aviador 139416-K*

Thesis for the degree of master in  
**Aeronáutica Militar, na Especialidade de Piloto  
Aviador**

## **Jury**

President:

Supervisor: Major/EngAer João Vieira Caetano

Member: Major/EngAer Luís Filipe da Silva Félix

**Sintra, May 2020**



## Acknowledgments

If you go alone, you will be faster, but if you really want to go further, you should better go together. This achievement was reached thanks to a group of people whom support and guidance was unquestionable through the making of this thesis.

Firstly, I want to make a special acknowledgment to my academic advisor for the constant support, readiness and motivation throughout this year. Without him, it would have been hard to overcome certain obstacles. Then, I would like to thank every single person that works at CIAFA for the help needed for the construction phase.

To all my family, especially my grandmother Maria José, my parents Paulo and Manuela, as well as my ever-little brother Afonso, for all the love, understanding and support during this course. Your vision, life lessons and caring, have given me the tools to pursue my dream, path and to always strain to be the best in everything I do.

To my beautiful, thoughtful and patient girlfriend Filipa. Thank you for being with me, even when I'm away. Your proud fuels my desire to go further, as well as to succeed.

Then, I would like to thank all "Distintos" for the support, experiences and camaraderie acquired during these 5 years spent with all of you.



## Abstract

In recent years, several studies were carried out in order to comprehend the complex flapping wing dynamics and aerodynamics, allowing for the creation of the very first nature inspired Flapping Wing Micro Aerial Vehicles (FWMAV). In the military field, Israel Aerospace Industries' Butterfly is one of the successful attempts to create a FWMAV capable of sustained flight.

In Portugal, this kind of drone propulsion is very rarely used. However, efforts have been made to study and create FWMAVs for future military empowerment. The fact that PAF does not have an indoor surveillance drone, motivated the development of this thesis, by improving an existing FWMAV, empowering it with the capacity of live video recording, as well as the ability to confuse the enemy by giving it a translucent aspect.

Before construction, a study was made in order to understand the aerodynamic principles of flapping flight. Then, several wings were developed and built, each one with different characteristics. By analyzing previous projects, the best suited materials were acquired. After the successful FWMAV construction, flight tests were carried out, in order to get a sustained and controlled flight. The intended objectives are: i) to assess the influence of aspect ratio and wing geometry on flapping frequency, lift generation ability and wing efficiency; ii) to improve flight stability by implementing structural modifications. iii) to install a FPV system capable of livestream. Then, data was obtained in order to compare with the different wings and check the improved performance.

In conclusion, the final objective on this thesis was achieved, by developing a FWMAV capable of flying while broadcasting live stream video with improved overall performance.



# Resumo

Nos últimos anos, vários estudos foram realizados de modo a compreender a complexa dinâmica e aerodinâmica do bater das asas, permitindo a produção dos primeiros Micro Veículos Aéreos de Bater inspirados na natureza, cuja sigla inglesa é FWMAV. No campo militar, a borboleta das indústrias aeroespaciais de Israel é uma das tentativas bem-sucedidas de criar um FWMAV capaz de realizar vôo sustentado.

Em Portugal, este tipo de propulsão em drones é muito pouco utilizado. No entanto, atualmente têm-se realizado esforços para estudar e criar FWMAVs para futura utilização militar. O facto de a FAP não possuir um drone de vigilância de interiores, motivou o desenvolvimento desta tese, através de um melhoramento de um FWMAV já existente, capacitando-o de uma câmara de gravação ao vivo, bem como a habilidade de confundir o inimigo, proporcionando-lhe um aspecto translúcido.

Antes da construção, foi realizado um estudo para entender os princípios aerodinâmicos do voo de bater asas. Em seguida, várias asas foram desenvolvidas e construídas, cada uma com diferentes características. Ao analisar projetos anteriores, os materiais mais adequados foram adquiridos. Após a construção do FWMAV, foram realizados testes de operação a fim de obter um vôo sustentado e controlado. Os objetivos pretendidos são: i) avaliar a influência da relação de aspeto e da geometria de asa com a frequência de batimento das asas, a produção de sustentação e com a relação impulso-potência; ii) melhorar a estabilidade de voo através da implementação de modificações estruturais. Em seguida, foram obtidos dados para comparar as diferentes asas, a fim de verificar e quantificar a evolução do desempenho.

Em conclusão, o objetivo final desta tese foi cumprido, através do desenvolvimento de um FWMAV de desempenho melhorado, capaz de voar enquanto transmite imagens ao vivo.





# Outline

List of figures.....	xi
List of formulas.....	xiii
Acronyms.....	xv
Chapter 1. Introduction.....	1
1.1. Background.....	2
1.2. Motivation.....	4
1.3. Objectives.....	5
1.4. Dissertation Structure.....	5
<b>Chapter 2. Literature Review.....</b>	<b>7</b>
2.1. Aerodynamic principles.....	8
2.1.1. Reynolds number.....	8
2.1.2. Fluid viscosity .....	9
2.1.3. Vorticity .....	9
2.1.4. Unsteadiness.....	10
2.1.5. Kutta condition.....	10
2.1.6. Circulation.....	11
2.2. Kinematics of Flapping Flight.....	12
2.3. Aerodynamic mechanisms of insect flight.....	14
2.3.1. Leading Edge Vortex.....	14
2.3.2. Wagner Effect.....	15
2.3.3. Rotational forces.....	15
2.3.4. Wing-Wake Interaction.....	16
2.3.5. Added Mass.....	17
2.3.6. Clap-and-Fling.....	18
<b>Chapter 3. Design optimization and construction.....</b>	<b>21</b>
3.1. Structural design.....	22
3.1.1. Structural design of the flapping mechanism.....	23
3.1.2. Structural design of the wings.....	24
3.1.2.1. Review of past developments.....	24
3.1.2.2. Wing development.....	26

3.1.3. Structural design of the tail.....	29
3.2. Electronics.....	31
3.3. Video streaming.....	33
<b>Chapter 4. Data analysis and comparison.....</b>	<b>37</b>
4.1. Lift generation and maximum payload.....	38
4.2. Flapping frequency .....	40
4.3. Endurance and efficiency.....	42
4.4. Influence of the Aspect Ratio.....	44
4.5. Stability and Control.....	46
<b>Chapter 5. Conclusions and Recommendations.....</b>	<b>49</b>
5.1. Conclusions.....	51
5.2. Recommendations and Future Work.....	53
<b>Bibliography.....</b>	<b>55</b>
<b>Annexes.....</b>	<b>59</b>

# List of figures

<b>Figure 1.1-</b> Wing designs for proposed flying machine by Leonardo da Vinci.....	3
<b>Figure 1.2-</b> DeIFly Nimble FWMAV project.....	3
<b>Figure 1.3-</b> Dissertation structure diagram.....	5
<b>Figure 2.1-</b> Airfoil moving through airflow.....	9
<b>Figure 2.2-</b> Illustration of the vortex vectors (Doswell, 2000).....	10
<b>Figure 2.3-</b> a) No Kutta condition (Zero lift); b) Circulation; c) Kutta condition established (Sane, 2003, p. 4195).....	11
<b>Figure 2.4-</b> Representation of a flapping wing kinematics, as well as eight-shape wing tip trajectory (Phillips, N, & Knowles, K., 2010).....	13
<b>Figure 2.5-</b> The red line represents a pear-shaped wing tip trajectory (Fritz-Olaf Lehmann and Simon Pick, 2007).....	13
<b>Figure 2.6-</b> Representation of LEV formation (Nabawy, Mostafa R.A. Crowther, William J., 2017).....	14
<b>Figure 2.7-</b> Wagner effect and the development of circulation (Sane, 2003)...	15
<b>Figure 2.8-</b> Wing wake production, and its interactions (Sane, 2003).....	17
<b>Figure 2.9-</b> Schematic representation of wing clap, when the airfoils meet each other (A-C), and then they fling apart (D-F). The black lines represent the flow, the dark blue arrows illustrate airfoil induced velocity, whereas light blue arrows show lift generation on the airfoil (Sane, 2003).....	19
<b>Figure 3.1-</b> Intended FWMAV configuration, built by Lobo Ferreira.....	22
<b>Figure 3.2-</b> Bruggeman (2010) flapping mechanism.....	23
<b>Figure 3.3-</b> Different wing shapes tested by (Bruggeman, 2010, p. 66).....	24
<b>Figure 3.4-</b> Different stiffener angles (Bruggeman, 2010, p. 62).....	25
<b>Figure 3.5-</b> Different aspect ratios tested (Bruggeman, 2010, p. 68).....	25
<b>Figure 3.6-</b> Table representing characteristics from several wings.....	26

<b>Figure 3.7-</b> 140mm wings with stiffener and section measurements (mm), not to scale.....	27
<b>Figure 3.8-</b> Tail design with stiffener and section measurements (mm) (not to scale): Top- Vertical stabilizer and Rudder; Down- Horizontal stabilizer and Elevator.....	30
<b>Figure 3.9-</b> FWMAV Improved tail.....	31
<b>Figure 3.10-</b> DelTangRx43d wiring for brushless motor output.....	33
<b>Figure 3.11-</b> ESC electrical wiring .....	33
<b>Figure 3.12-</b> Receiver Signal Process .....	34
<b>Figure 3.13-</b> Fatshark Dominator V3 FPV system .....	35
<b>Figure 3.14-</b> 5.8GHz 40ch FPV Camera.....	35
<b>Figure 3.15-</b> 150mah battery with additional connector.....	35
<b>Figure 4.1-</b> Maximum lift test, where small weights are added.....	38
<b>Figure 4.2-</b> Lift generation test in order to calculate maximum lift capability (orange) and payload (grey), depending on drone's weight (blue).....	39
<b>Figure 4.3-</b> Bruggeman (2010, figure 5.2.2, p.69) graphics of different AR wings, relating flapping frequency, thrust and power.....	40
<b>Figure 4.4-</b> Flapping frequency test.....	41
<b>Figure 4.5-</b> Graphic illustrating the flapping frequency test, where the maximum flapping frequency (orange) of each wing is represented.....	42
<b>Figure 4.6-</b> Swirling strength at the end of the out-stroke (E), halfway during the in-stroke (I) and at the end of the in-stroke (L) for the 140mm wing. Showing leading edge vortices (LEV) and trailing edge vortices (TEV). (M.A. Groen, 2010).....	45
<b>Figure 4.7-</b> Swirling strength at the end of the out-stroke (A), halfway during the in-stroke (B) and at the end of the in-stroke (C) for the high aspect ratio wing (M.A. Groen, 2010).....	45
<b>Figure 4.8-</b> FWMAV component setup.....	47

# List of formulas

## **1 – Reynolds Number:**

- .  $\rho$  - fluid density;
- .  $U_\infty$  – relative fluid speed;
- .  $L$  – surface length;
- .  $\eta$  – dynamic viscosity.

## **2 – Aspect Ratio:**

- .  $R$  – span;
- .  $S$  – area.

## **3 – Relation between Reynolds Number and Aspect Ratio:**

- .  $\varphi$  - stroke angle;
- .  $R$  – length;
- .  $\nu$  - kinematic viscosity;
- .  $\eta$  - flapping frequency.



# Acronyms

AOA	Angle of Attack
AR	Aspect Ratio
CIAFA	Centro de Investigação da Academia da Força Aérea
COG	Center of Gravity
ESC	Electronic Speed Controller
FAP	Força Aérea Portuguesa
FPV	First-Person View
FWMAV	Flapping Wing Micro Aerial Vehicle
LEV	Leading Edge Vortices
MINUSCA	Missão Multidimensional Integrada das Nações Unidas para a Estabilização da República Centro-Africana
NATO	North Atlantic Treaty Organization
NSPA	NATO Support and Procurement Agency
PAF	Portuguese Air Force
TEV	Trailing Edge Vortices
UAV	Unmanned Aerial Vehicle





# Chapter 1. Introduction

---

In this chapter, a reference about human interest in animal flight will be made, as well as the beginning of aviation history and its evolution. Then, some advances around the flapping mechanism will be displayed, making it a starting point for this dissertation. By analyzing the needs of the PAF and the global tendency for military-drone's advances, a motivation for the execution of this project and its purpose will be referred. A starting question will then be outlined, defining the intended objectives for the embodiment of this thesis. To finish, the structure of the dissertation will be presented.

## 1.1. Background

Flight is a process of locomotion used by several species in order to migrate, feed and escape from predators. This act became more efficient and widespread thanks to the adaptability and evolution of flying species. It is believed that its genesis dates back to the Carboniferous period, approximately 300 million years ago. By that time, dragonfly ancestral like the 70cm wingspan *Meganeura* dominated the air, having no predators and therefore demonstrating the benefits of flying.

Since the beginning of mankind men have always been mesmerized by every flying species that existed. There was a constant need to understand their movements and characteristics, in order to reproduce the same exact flight. Several bold and genius people went down in history after making endeavors in this area, like the legend of Icarus and Daedalus [Graves, 1955], and during Renaissance with Da Vinci (Figure 1.1). He found inspiration in birds and bats, allowing him to design flying machines that would later be built and tested. One of his designs was used by João Torto whilst jumping off a church, not being able to hover for a long distance and resulting in fatality (**Lapa, 1928**). One misjudged aspect in these designs was the power-to-weight ratio, turning out to be impossible to flap wings with the arms.

The first successful flight machine was lighter than air balloons, during the 17th century with Galileo's experiments in which he showed that air had weight, so he could change its density in order to obtain lift. Nevertheless, only on December 17<sup>th</sup> 1903 did man fly in a heavier-than-air aircraft, the Wright Flyer. This machine was powered by a petrol engine, which span a propeller, thus generating thrust. However, lift was produced by fixed wings, which were unable to flap. Until the last century, men have always overlooked the animal flight potential, and the perks that could arise from it. Nowadays, progress is being made in robots that mimic insect and bird flight movements for intelligence and reconnaissance missions, when there is high risk for the troops involved.

Internationally renowned universities like David Lentink's laboratory in Stanford, are trying to understand every aspect of biological flight through biofluid dynamics and other quantitative engineering disciplines, including robotics, as

research tools to understand and embody animal flight performance. According to **Caetano (2016)**, three strategies can be taken in order to analyze animal flight: 1) The first strategy aims to study flying species in a confined space, providing significant data upon aerodynamics and kinematics of flapping flight, e.g. **Weis-Fogh (1972, 1973, 1975)**. Subsequently, the second strategy combines aerodynamic, kinetic and inertial principals to design a computer simulation modeling of flapping wings systems, like **Miller and Peskin (2005)**. At last, the production and data monitoring of FWMAV is taken into course, with the purpose of optimizing and creating different flight mechanisms thanks to the advances in this area. One example is DeIFly II Flapping Wing Micro Aerial Vehicle (FWMAV) from **Caetano et al. (2015)** in partnership with the Delft University of Technology, or more recently the DeIFly Nimble FWMAV (Figure 1.2), capable of performing high degree turns like flies.

The objective of this thesis is to improve FWMAV capabilities by studying several wings with different characteristics and then comparing their performance according to some key aspects (lift production, flapping frequency and wing efficiency), as well as modifying both materials and structure to improve flight stability and control. Thus, it has to be capable of video live streaming.

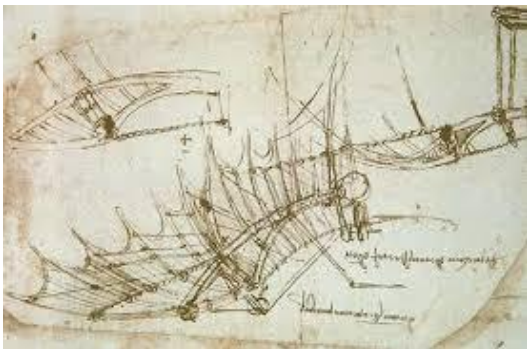


**Figure 1.1** - Wing designs for proposed flying project machine by Leonardo da Vinci.



**Figure 1.2** - DeIFly Nimble FWMAV

## 1.2. Motivation

Throughout the history of war there is a tendency to attack without being compromised, by allowing space between opponents, and consequently losing physical contact from then on. Technology has taken place in the battlefield, as troops started to realize they could inflict damage while remaining safe. Several civil organizations, as well as military like NATO, are starting to become interested in acquiring and developing drones that could perform complex tasks and assist military forces, seeking several advantages like less risk involved and longer operation times without wearing out personnel. (**Ferreira, 2018**)

Nowadays, Unmanned Air Vehicles (UAV) are a reality amongst almost all Armed Forces, carrying out varied missions such as providing ground and aerial gunnery with a target that simulates an enemy aircraft, obtaining battlefield intelligence or even increasing attack capability for high-risk missions. In Portugal, efforts are being made to promote and employ these systems, like the Mini-UAV's Raven B Digital Data-Link acquired by NATO Support and Procurement Agency (NSPA), presented this year in the Nr.5 Artillery Regiment near Vendas Novas. According to the National Defense Minister João Gomes Cravinho, this UAV is now taking part on the United Nations Multidimensional Integrated Stabilization Mission in the Central African Republic (MINUSCA). This was a desired objective underlined in the Military Programming Law in 2015 for the Portuguese Army.

However, these types of drones are only suitable for outdoor surveillance, as its fixed wings only obtain lift due to airspeed. FWMAV, which resemble animal flight, are the future of close-range support and indoor reconnaissance, thanks to its flapping wing movement. It allows the flight inside buildings that could present a serious hazard for people. Portugal would benefit from this technology, as it would increase the operability and field of action of the armed forces (**Ferreira,2018**). The academic research along with the Portuguese Air Force Academy Investigation Centre (CIAFA), would definitely increase the skills and understanding on how to operate and produce FWMAV.

The key question of this thesis is:

**“How to develop a flapping wing micro air vehicle with live streaming capabilities”?**

### 1.3. Objectives

This dissertation has the purpose of designing, building and improving a Flapping Wing Micro Air Vehicle capable of transmitting a first-person-view video. Hence, it should be capable of a stable and controlled flight for at least 4 minutes. The FWMAV should be controllable via radio, and have the freedom to move around a 3-dimensional space.

Moreover, it has to be light, affordable and simple to build and rebuild in case of accident.

### 1.4. Dissertation Structure

The subsequent thesis is divided into several stages. Each of them has various sub-topics that are vital for the study and development of this FWMAV.

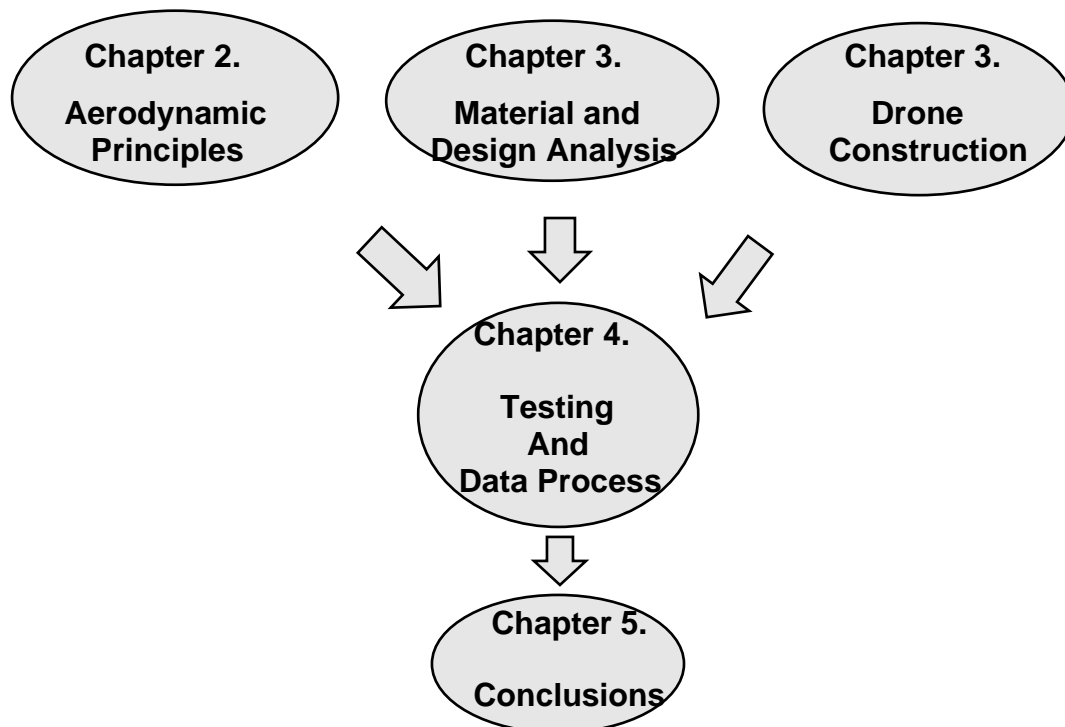


**Figure 1.3-** Dissertation structure diagram.

- **1<sup>st</sup> chapter**

This chapter introduces the fundamentals for the elaboration of this dissertation, retrieving the origins of flapping flight. Moreover, the motivation for the FWMAV development is also presented, as well as the desired objectives. A brief explanation of the thesis structure is made, by providing an insight of the different chapters.

- **2<sup>nd</sup> chapter**

This chapter addresses the aerodynamic principles and fundamentals of flapping flight, revealing all the phenomena behind flapping flight kinematics. A revision about the flapping aerodynamic principles is made, explaining how they will affect the flapping flight system and therefore the overall performance and behavior of the FWMAV.

- **3rd chapter**

This chapter makes an in-depth analysis of the components needed and the suitable materials. Then, the structural design of the several parts will be explained based on studies made and the intended upgrades. Subsequently, the electronics will be selected.

- **4th chapter**

This chapter shows all of the different tests carried out in order to choose the best wing setup as well as stability and control improvements. Moreover, its flight capabilities will be assessed by explaining the advantages that some wings have due to geometric shape.

- **Conclusion**

By way of conclusion, the drone improved performance is quantified and compared with previous FWMAV, therefore assessing the progress made in the field. The accomplished objectives are underlined, the difficulties encountered are explained and some considerations for future studies are made.

## Chapter 2. Literature Review

---

This chapter details the theoretical background needed to support the study and discussion of the thesis. Micro UAV operation and the aerodynamic principles behind flapping wing movement will be discussed, along with an understanding of the kinematics of flapping flight.

## 2.1. Aerodynamic principles

Flapping wing aerodynamics differs from a conventional wing, which produces its lift from the airspeed that passes by it, creating a pressure differential and resulting in an upward force. It is indeed a more complex phenomena that gathers several principles that will be explained below.

### 2.1.1. Reynolds number

When an object crosses the atmosphere, the air molecules near the object are disturbed and move around it, thus creating aerodynamic forces. Reynolds number is a dimensionless figure that expresses the ratio between inertial forces and viscous forces, allowing for a better understanding of the air flow behavior when it meets the wing.

Reynolds number can be calculated through the following equation:

$$Re = \frac{\rho U_{\infty} L}{\eta} \quad (1)$$

Where the  $\rho$  is the fluid density,  $U_{\infty}$  is the relative fluid speed approaching the object,  $L$  being the length of the object surface and  $\eta$  the fluid's dynamic viscosity.

High Reynolds number means viscous forces are small, so that the flow will stick to the wing creating a laminar flow through it. Whereas Low Reynolds number means viscous forces should be considered, creating more turbulence due to the increased air resistance. Nonetheless, the flow becomes turbulent when the Reynolds Number is high.

Reynolds Number is a fundamental aspect of flapping wing aerodynamics, as it predicts the type of flow created on the airfoils, enabling us to use the correct equations for the airfoil in study. As it is a dimensionless number, it is useful to predict the behavior of a real size object, by studying a scale model, i.e., small size with the same proportions.



### 2.1.2. Fluid viscosity

Viscosity is defined as the amount of resistance measured when there is a shear force acting on a fluid, causing it to deform. In other words, it is the internal friction created inside the fluid. The higher the resistance measured, the larger the viscosity. In any given flow, every fluid has to undergo with no slip condition, having zero velocity at the surface of contact with respect to a moving object.

In the case of an airfoil (Figure 2.1), if the angle of attack is increased, the airflow will become turbulent after the transition point, detaching from the wing surface. This effect will be increased if Reynolds number is low, meaning a high fluid viscosity, therefore increasing turbulent air flow formation closer to the leading edge. This disturbed air flow will interact with the boundary layer, which defines the separation between the undisturbed airflow and the flow influenced by the airfoil, creating a resistance force known as drag (D).

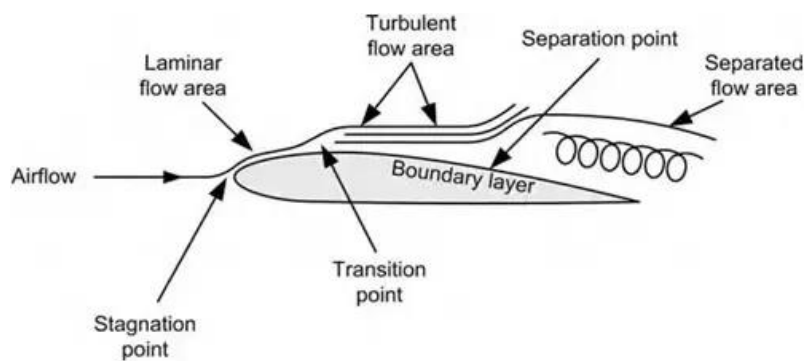
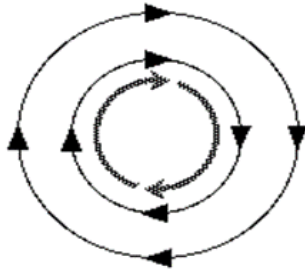


Figure 2.1– Airfoil moving through airflow.

### 2.1.3. Vorticity

According to **Holton J. R. (1979)**, vorticity is a vector field (Figure 2.2), which gives a microscopic measure of the rotation at any point in the fluid. This phenomenon is the underpinning of lift force production in FWMAV. As an inherent trait of a vector field it has, therefore, the same direction as the axis of rotation of the fluid (**Parker, 2001**), i.e., vortex is fluid rotating around its own axis, hence having linear and angular momentum. It loses energy when increasing the distance from the vortex center and due to viscous forces.



**Figure 2.2** - Illustration of the vortex vectors (Doswell, 2000).

#### 2.1.4. Unsteadiness

Flapping flight is characterized by aerodynamic interactions between insect wing surfaces and surrounding flow, generating local time-dependent changes in the flow field and aerodynamic load on the wings. This type of flight differs from a conventional airfoil behavior, whose force loads are time independent. This explains the contrast between them: “Within the context of force and flow dynamics, the term ‘steady’ signifies explicit time independence, whereas the word ‘unsteady’ signifies explicit temporal evolution due to inherently time-dependent phenomena within the fluid.” (*Sane, 2003, p. 4193*). However, in flapping flight quasi-steady models are often used, which take into account time-independent forces. According to *Sane (2003)*, despite these forces being constant over time, they still depend on the instant of kinematic motion.

#### 2.1.5. Kutta condition

Kutta condition is a phenomenon responsible for lift generation. On any given sharp corner of an airfoil, there is always a small radius of curvature, hence creating a stagnation point on either the leading and trailing edges. This means that they are points with zero fluid velocity. With a high AoA or at slow speeds (no lift capability), there is one stagnation point underneath the leading edge, and another one above the trailing edge (Figure 2.3a). This last one is responsible for creating a circulation that gets decoupled from the airfoil, originating a starting vortex.

Once the airfoil increases its speed or decreases its AoA, a circulation opposite to the one on the starting vortex is created (b), moving the stagnation points to the opposite direction. The stagnation point on the rear is therefore moved backwards, matching the trailing edge. Having lost its circulation, the upper and lower layer of the fluid can now merge together, hence establishing Kutta condition (c).

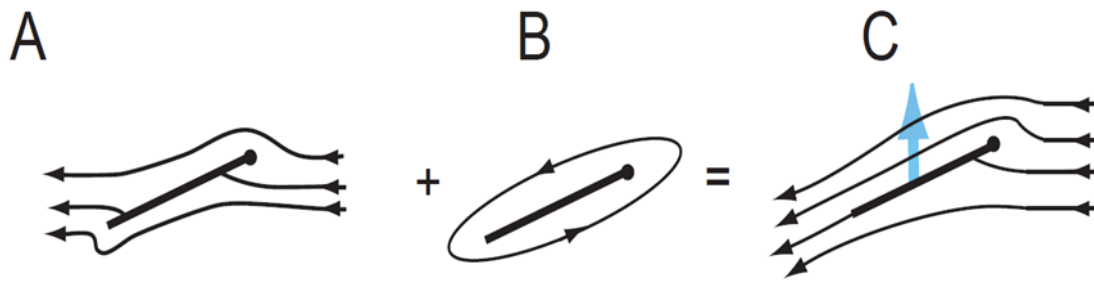


**Figure 2.3** - a) No Kutta condition (Zero lift); b) Circulation; c) Kutta condition established (Sane, 2003, p. 4195).

## 2.1.6. Circulation

Just like vorticity, circulation is a fluid movement induced by an airfoil, whose behavior depends on the fluid viscosity. It is a scalar quantity defined as the line integral of the velocity field along a closed contour, whereas vorticity is the curl of the velocity field.

They are both primary measures of rotation in a fluid, the main difference lies on the location where it occurs. Circulation refers to the moving flow around the airfoil, whereas vorticity applies to the flow that is created by the moving surface.

Placed in the context of this thesis, circulation is referred to as the rotational flow movement inside the boundary layer, which is responsible for the establishment of the Kutta Condition, as addressed before.

## 2.2. Kinematics of Flapping Flight

Flying species adopted several kinds of flapping kinematics, as well as different wing shapes, depending of their habitats, source of energy and predator hazards. Therefore, their evolution will result in the optimization of several aspects, like flight speed, wing shape, flapping frequency, hovering capacity, or flight time.

This assortment of flapping kinematics can be complex to analyze, as **Norberg (1975)** refers, parameters like flapping frequency, wing form and its structure, aspect ratio, wing flexibility differ considerably amongst species.

When talking about studies on flapping of small species, we are mostly talking about hovering, since it is easier for researches to calculate the balance between lift and weight (**Sane, 2003**). Insects have different kinds of wing trajectories, as some of them move their wings back and forth creating a horizontal line, while others lean themselves forward resulting in an oblique stroke plane (**Ellington, 1984c; Dudley, 2000**).

By analyzing flapping wings kinematics, three main movements can be described:

- Heaving motion/plunging ( $\theta$ ), representing the horizontal wing movement around Z axis. This motion is only present in some species, defining wing tip trajectory, therefore being a variable, conditioning the lift force produced (**Sane & Dickinson, 2001**). According to **Perçin (2015)**, it is possible to observe two kinds of trajectories: an eight-shaped wing tip trajectory (Figure 2.4), where wing tip trajectories intercept each other during downstroke and upstroke; and a pear-shaped pattern (Figure 2.5).
- Sweeping motion ( $\phi$ ) is defined by the stroke angle, i.e., it is the maximum wing deflection around the X axis represented on Figure 2.4. This movement is composed of two stages: the upstroke, when the wing moves backwards, reaching the maximum stroke angle ( $\phi$ ); the downstroke, when the wing moves forward. These two stages are connected by two

transitions: pronation, when it changes from upstroke to downstroke, and supination, when it shifts from downstroke to upstroke.

- Pitching motion ( $\alpha$ ) refers to the wing angle performed around the Y axis of the wing. This angle has an influence in the lift force generated, depending on the flapping and pitch rate, the rotation axis position and rotation timing. It is commonly performed during stroke reversals, so it can have a positive AoA in following stroke.

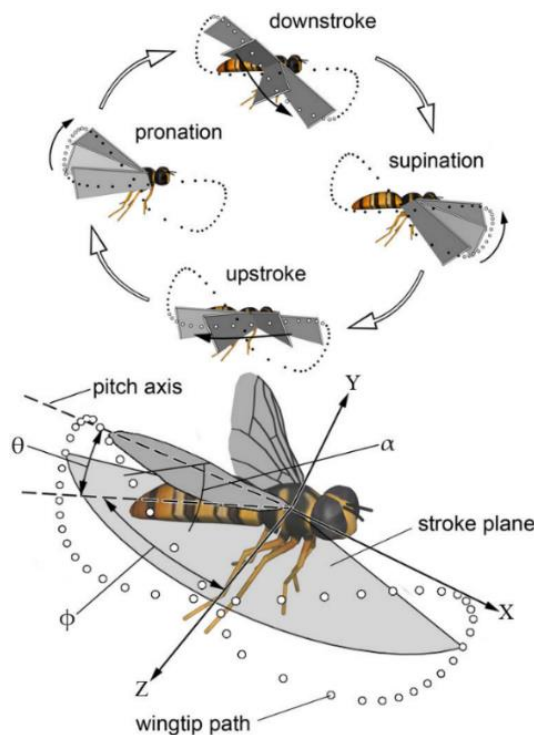


**Figure 2.4** - Representation of a flapping wing kinematics, as well as eight-shaped wing tip trajectory (Phillips, N, & Knowles, K., 2010).

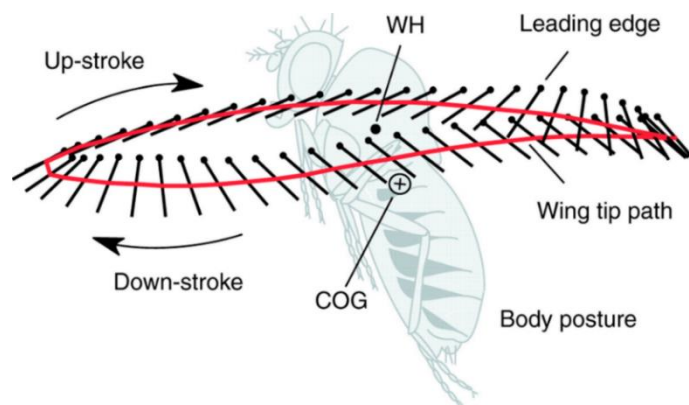


**Figure 2.5** - The red line represents a pear-shaped wing tip trajectory (Fritz-Olaf Lehmann and Simon Pick, 2007).

## 2.3. Aerodynamic mechanisms of insect flight

After explaining the kinematics of flapping flight and the fundamentals of aerodynamics, it is then time to expand our knowledge about the intricate flapping-wing system's aerodynamics. These phenomena considered as unsteady forces, are according to **Caetano (2016)**, the most important aerodynamic principles of flapping flight, and consequently the ones that will be reviewed.

### 2.3.1. Leading Edge Vortex

A leading-edge vortex (LEV) is formed on the leading edge of wings moving at high angles of attack, which grows in size and strength until it eventually sheds from the wing with a resulting loss of lift. The flow over the upper surface of the wing separates at the leading edge and then reattaches before the trailing edge, thus creating a low pressure zone, e.g. Figure 2.6(a).

A wing with a stable LEV is thus able to satisfy the Kutta condition at the trailing edge at angles of attack beyond which normally a stall would occur for wings where no LEV is present, and consequently a substantial improvement of the wing lift coefficient is achieved. Insects use this mechanism in certain conditions for a stable flapping flight (**Polhamus (1971); Ellington et al. (1996) and Dickinson et al. (1999)**).

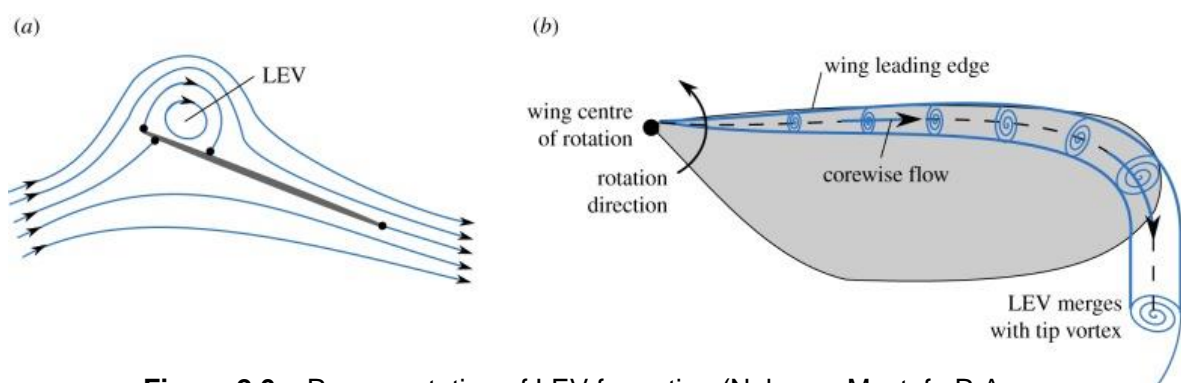


**Figure 2.6** – Representation of LEV formation (Nabawy, Mostafa R.A. Crowther, William J., 2017).

### 2.3.2. Wagner Effect

This effect, originally proposed by **Wagner (1925)**, explains the delayed growth of circulation once the wing is accelerating from a stand still position, therefore holding back the steady-state and the subsequent generation of lift. This effect is due to two factors (**Sane, 2003**): i) The first one is the delayed establishment of the Kutta condition on account of the viscous action of the fluid; ii) The second one is the opposite rotation of the starting vortex created by the velocity field in the trailing edge, thus suppressing the circulation growth. This effect is illustrated in Figure 2.7, where the circulation is heightened once the trailing edge vortex moves away from the airfoil.

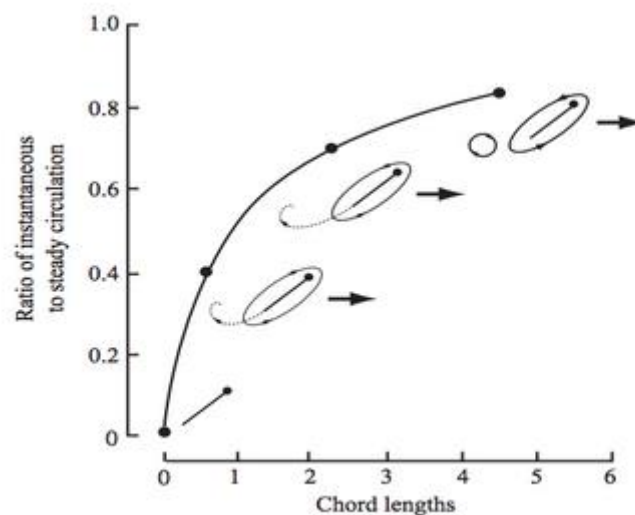


**Figure 2.7** - Wagner effect and the development of circulation (Sane, 2003).

### 2.3.3. Rotational forces

Sweeping motion is characterized by the flapping wing movement, keeping a high pitch needed to spawn LEV. Once the wing performs its downstroke movement and reaches its maximum forward/low limit, a rotation of the wing is required in order to start the new sweeping motion with a positive angle of attack. By the time it reaches the point of stroke reversal, there is a sudden rotation, thus creating rotational forces. This rapid wing movement will move the stagnation point away from the trailing edge, halting the establishment of the Kutta condition (**Perçin, 2015**).

In order to continue lift production, this condition has to be present continuously, therefore existing an effect that counteracts trailing edge shear and wake. It was initially called Kramer effect, identified by **Kramer (1932)** and referred as rotational circulation (**Dickinson et al., 1999**) afterwards. This phenomenon is based on an opposite circulation force created by fluids viscosity, capable of reestablish Kutta condition and lift generation capability (**Sane, 2003**).

**Dickinson et al. (1999)** and **Sane and Dickinson (2002)** experimentally confirmed that the rotation could generate or wane lift, depending on the position of the rotation axis and its timing. Circulatory force will be beneficial if the rotation is in the direction of an increase in the angle of attack; whereas, it has an opposite effect if the wing pitches down during rotation.

#### 2.3.4. Wing-Wake Interaction

Flapping wing systems, contrarily to fixed-wing that only generate lift from laminar and steady flow, are capable to operate in turbulent and disturbed air. Due to the low advance ratio, the wing has to flap repeatedly around the same position, therefore coming up with sheds both the LEV and the trailing edge vortices from the previous stroke.

This effect, called Wing-Wake interaction, will enhance the generated forces due to a positive addition of locally induced velocities. **Dickinson et al. (1999)** also proved a relation between the advance of wing rotation during stroke reversal and the amount of wake produced, in Figure 2.8. From A to C, the wing is shedding both leading and the trailing edge vortices, which induce a strong inter-vortex velocity field. Once in stroke reversal, sub fig. D to F, the wing encounters the induced velocity fields, thus resulting in a great aerodynamic force generation.



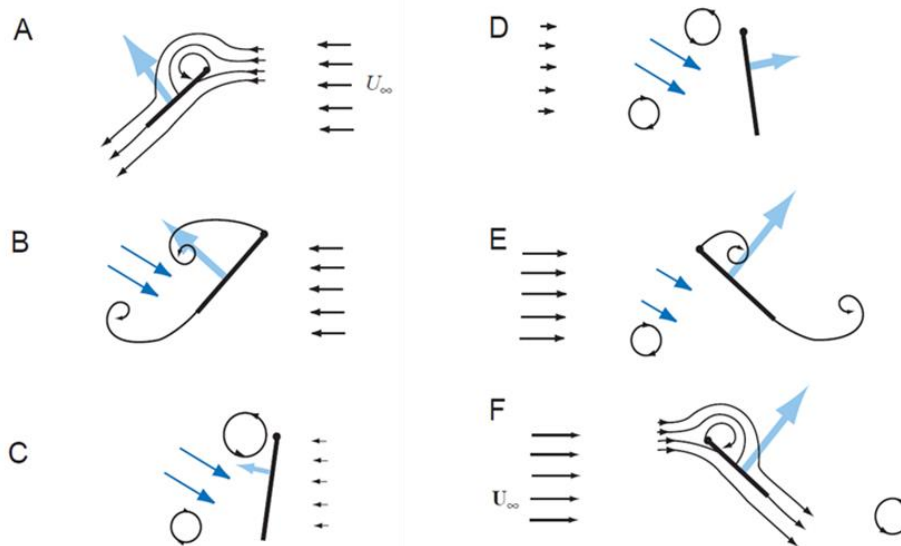


**Figure 2.8** - Wing wake production, and its interactions (Sane, 2003).

### 2.3.5. Added Mass

According to the 3rd Newton Law, for every action there is an equal and opposite reaction. This happens when a wing flaps and accelerates the surrounding fluid, thus applying pressure against the fluid mass, ending up with an opposite force, known as 'virtual mass', described by **Ellington (1984)**.

Unlike other circulatory forces whose action can be mathematically calculated and analyzed due to changes in the velocity potential around the wing (see 2.1.1,2,3,4), this is a non-circulatory reactive force, as **Sedov (1965)** describes. Once it coexists with the remainder circulatory forces, it has several components emerging from rotational acceleration, as well as from translational velocity and angular velocity (**Ellington, 1984d**), therefore being difficult to calculate and identify. It is possible to estimate the magnitude of added mass, by comparing the ensemble of all the forces acting on the airfoil, with the amount of contribution of circulatory forces, accomplished by **Sane and Dickinson (2002)**.

### 2.3.6. Clap-and-Fling

Also known as the Weis-Fogh mechanism, this effect was proposed by **Weis-Fogh (1973)** in order to explain the lift enhancement of several flying insect species. It can be separated in two movements:

- i) The clap (Figure 2.9A-C), when the wings pronate to start the downstroke. Firstly, leading edges gather, conveying the movement until reaching the trailing edges. This will close the gap between them, expelling the air downwards. Secondly, trailing edge vortices will be faded out in the next stroke, thus stopping circulation delaying and preventing Wagner effect. According to **Weis-Fogh (1973)** and **Lighthill (1973)**, this attenuation would allow the wings to extend the benefit of lift, by building up more circulation from stroke to stroke.
- ii) The fling (D-F), consisting on the separation and upstroke movement of the wings. Consequently, leading edges start to detach, creating a gap between the wings, thus generating a low pressure inside it. Moreover, this action will trigger an increased vorticity, as well as a leading-edge vortex intensification. This means more circulation around the wings, therefore resulting in a lift generation.

Although “Clap-and-Fling” is applicable to a rigid wing, proves to be a useful effect to significantly increase lift, it was proven according to **Ellington (1984b)**, that flexible wings can contribute to a greater enhancement of the forces created. This phenomenon is called “Clap-and-Peel”, and in spite of having the same movement, the wings will have a smaller AoA between them, enabling a greater suction as well as a LEV enhancement, therefore lowering drag and creating even more lift.

Studies also suggest that flexible wings tend to reduce the starting vortex, i.e. Wagner Effect, allowing circulation around the wing, therefore permitting Kutta condition to be established, as well as, increasing lift generation (Sane, 2003).

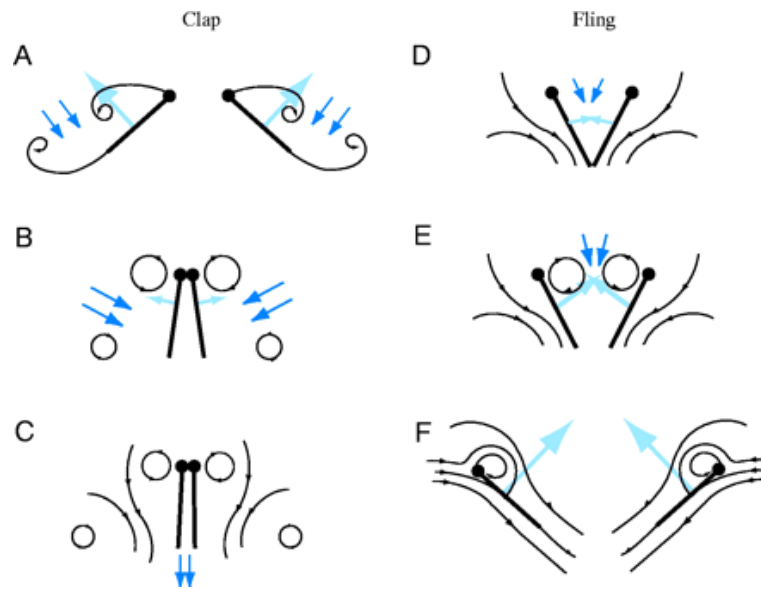


**Figure 2.9** – Schematic representation of wing clap, when the airfoils meet each other (A-C), and then they fling apart (D-F). The black lines represent the flow, the dark blue arrows illustrate airfoil induced velocity, whereas light blue arrows show lift generation on the airfoil (Sane, 2003).



## Chapter 3. Design optimization and construction

---

The purpose of this chapter is to discuss the parts that aim to be upgraded based on the established requirements. A detailed explanation about several of the component changes will be made, namely wings, tail, flapping mechanism and electronics. In regard to the wings, a review of past developments will be made, as well as addressing the development and construction. Brushless engine's mechanics will be presented, and livestream video transmitting system explained.

### 3.1. Structural design

Before creating a FWMAV, a design has to be chosen based on its function and the materials available. Given that the primary purpose of this drone is indoor surveillance, the criteria is based on the stability and control, since it has to record video footage.

In order to get a statically and dynamically stable drone, a tail has to be present (**Ferreira, 2018**). This component helps to counteract the existing moments that are generated by the wings, enabling the return to a balance point. Hence, this would create the possibility to control the FWMAV with surface controls, namely rudder and elevator. The lift would then be produced only by the wings, allowing for a simpler flapping mechanism design with one-degree of motion.

According to **Ferreira (2018)** and after analyzing his structural design comparison, a biplane FWMAV seems to be the best choice, since it has a lower power consumption than a monoplane due to Clap-and-Fling effect explained on section 2.3.6. This phenomenon is able to increase lift generation by 25% while maintaining the same clap rate (**Marden, 1987**). Furthermore, there is an absence of unstable moments as well as flapping oscillations due to symmetric wing design and operation.

By choosing a biplane configuration with a tail (Figure 3.1), there could be a great weight reduction, as it avoids unnecessary electronics like sensors as well as a wing mechanism enabling several degrees of freedom.

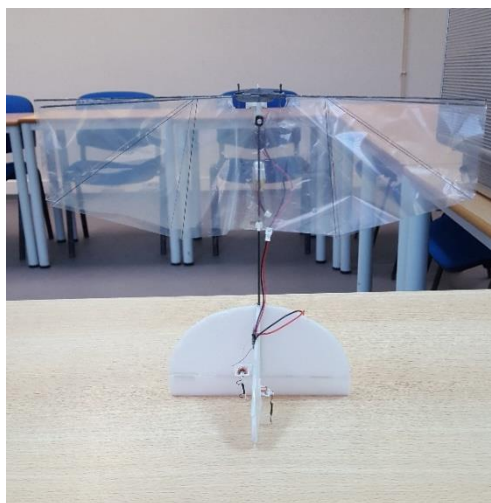


**Figure 3.1** – Intended FWMAV configuration, built by Lobo Ferreira.

### 3.1.1. Structural design of the flapping mechanism

The flapping mechanism is the most complex system in the FWMAV, responsible for transmitting the motor's rotation to the wings, through gears. This is accomplished by connecting the motor to the frame, linked to a gear. Its rotation will move the intermediate gear, which will transfer the motion to the main gears connected to the wings. This connection is made by pushrods, transforming rotational for linear movement. The leading-edge rods would then be attached to the flapping connectors, thus enabling wing movement.

Throughout this entire process, the motor rotation should be slowed down until it is transferred to the wings, thanks to larger gears. It is called gear ratio, and it ensures that the flapping frequency stays between 10-20Hz, the interval in which the FWMAV is able to hover (**Caetano, 2016**). Less than 10Hz, there is not enough lift being generated. Conversely, more than 20Hz, could promote a structural failure on the flapping mechanism and wings.

The flapping mechanism has to be light and resistant enough to withstand the high rotations generated by the motor. It also has to be built with precision, in order to avoid wear and friction that would then decrease the power output.

Producing such mechanism would mean special equipment, as well as being too time consuming. Therefore, it is not part of our plan to try to design our own flapping mechanism. Consequently, using Bruggeman's flapping mechanism was considered (Figure 3.2). It has proved to be a valuable option, since it was used on DelFly project (**Delft University of Technology, 2017**) and a similar one on Berkeley's  $H^2$  Bird.

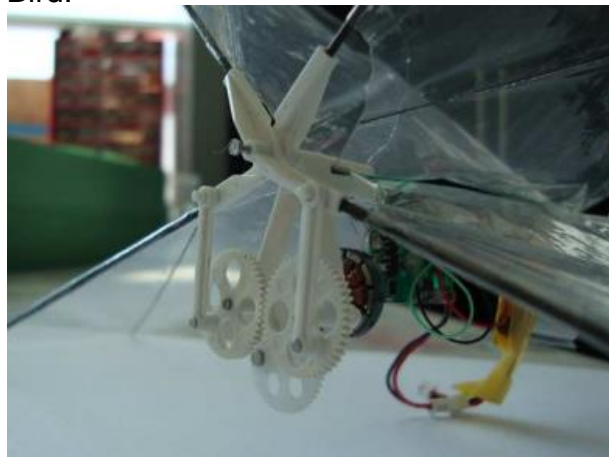


**Figure 3.2** - Bruggeman (2010) flapping mechanism.

### 3.1.2. Structural design of the wings

#### 3.1.2.1. Review of past developments

Regarding wing design, the best choice tends to fall upon a configuration with the highest thrust-to-power ratio. Not only this, but the preferred solution aims for a design that has been studied and experimentally proven by detailed scientific work. Hence, **Bruggeman's (2010)** dissertation was reviewed, where several aspects such as wing shape, aspect ratio and stiffener positions were analyzed.

In Figure 3.3, three wing designs tested by Bruggeman are presented, namely Normal, Bat-like and Reversed.

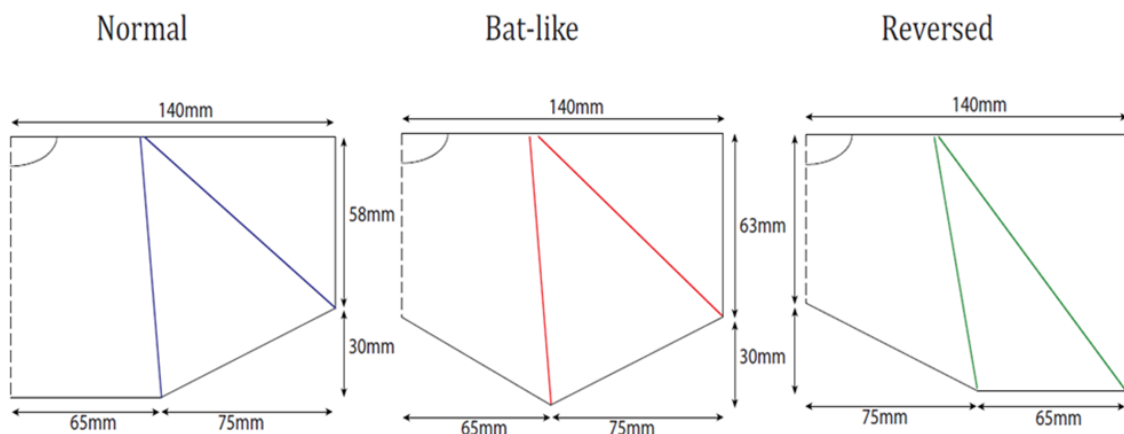


**Figure 3.3** - Different wing shapes tested by (Bruggeman, 2010, p. 66).

He intends to know the influence of different wing area distributions on efficiency and thrust generation. The results showed that the bat-like wing had the best thrust-to-power ratio, since it required less energy to create the same amount of thrust than other wings. However, the normal wing proven to have a higher lift generation. Based on this investigation, the normal wing shape will be considered. With regard to stiffener position and orientation, Bruggeman tested several wings with different stiffener angles between them, as shown in Figure 3.4, also trying various stiffener lengths and thickness, modifying wing's ability to Clap-and-Peel. After carrying out lift generation tests, the wing 8435 achieved about 0.005N more thrust than the others. In respect to power consumption, this wing holds advantages, measuring more 5%±1% thrust-to-power ratio than the



standard wing from Delfly II (**Bruggeman, (2010)**). These gains are due to a smoother rotational phase (**M.A. Groen (2010)**).

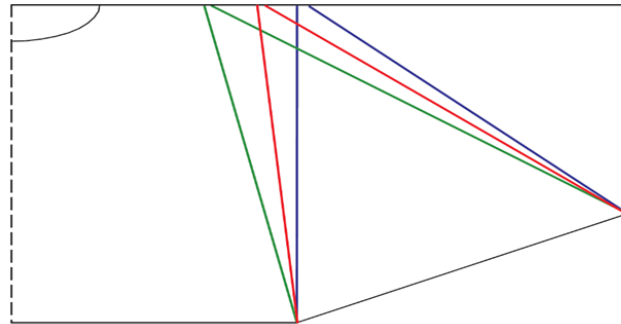


**Figure 3.4** - Different stiffener angles (Bruggeman, 2010, p. 62).

With respect to stiffener thickness, Bruggeman tested diameters ranging from 0.28mm up to 1.0mm. The wing deformation turned out to be inverse with the thickness increase. Moreover, thrust and power consumption increased when testing the biggest diameters. The additional weight also affected thrust-to-power ratio, since the motor had to cope with more inertia. Therefore, the 0.28mm diameter stiffeners proved to have better characteristics (**Bruggeman, (2010)**).

The aspect ratio was also tested (Figure 3.5), resulting on a higher thrust from the biggest aspect ratio wing, although consuming more energy. Consequently, the 1.75 AR wing demonstrated to have a higher thrust-to-power ratio, hence balancing thrust and consumed energy.

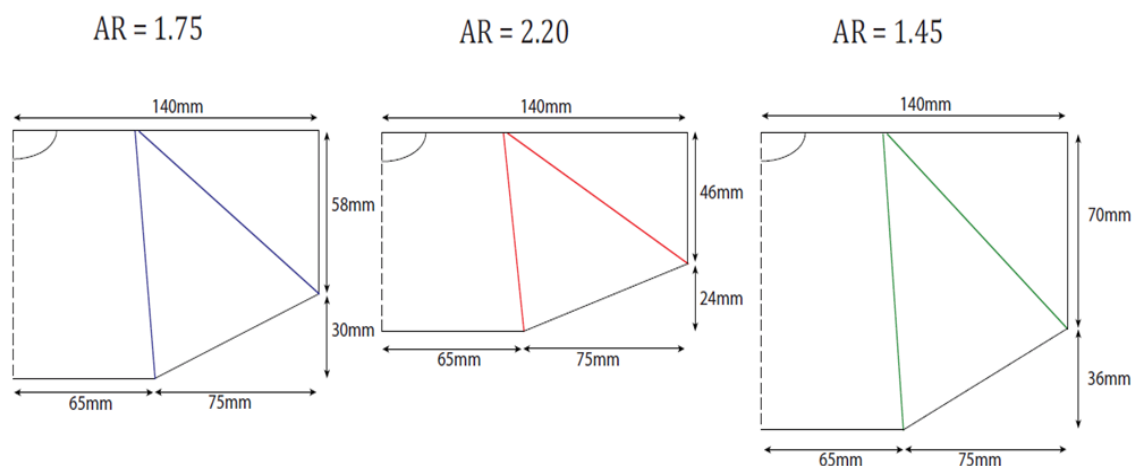


**Figure 3.5** - Different aspect ratios tested (Bruggeman, 2010, p. 68).

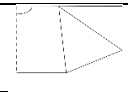
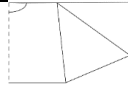
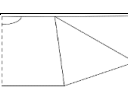
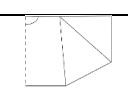
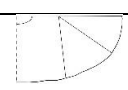
After determining the optimal specifications, the most suitable would be an 8435 wing with a normal configuration and an aspect ratio of 1.75. With regard to the thickness of stiffeners, they would comprehend between 0.28 and 0.5mm.

**Ferreira (2018)** then chose to develop three different size wings to scale, with a wingspan of 140, 119 and 98mm, as he didn't know whether the lack of power on his brushed motor would prevent it from hovering. Consequently, he realized that the 140mm wing was the one that had the most lift capability. As a more powerful motor will be used, the biggest wings should prevent the flapping frequency of increasing, as well as producing more lift, even with the extra weight. At least, it is what we can assume from the previous thesis.

**Perçin (2015)**, on *Aerodynamic Mechanisms of Flapping Flight* refers: "In terms of wing geometry, the study mainly focuses on the effect of aspect ratio for varying span lengths, which has not been considered in the previous studies and remains relatively unexplored." (p.64, chapter 3.3). Hence, in order to extend this research, more wings were produced, trying to understand the effect that different chord and span have on wing dynamics.

### 3.1.2.2. Wing development

In order to find the best wings that can suit the FWMAV needs, some tests were carried out with five pairs of wings, each one with different size and shape (Figure 3.6). By analyzing flapping frequency, endurance and maximum lift, the wings that perform better will be installed on the FWMAV. The wings were: 1- a standard 140mm wing, 2- a 15% proportionally bigger than the 140mm wing, 3- a larger aspect ratio wing with a span of 160mm, 4- a less span 119mm and 5- an elliptical 140mm wing.

Wing	Span	Chord	AR	Shape
1	140	89	1.78	
2	160	102.35	1.77	
3	160	89	2.05	
4	119	89	1.49	
5	140	89	2.05	

**Figure 3.6-** Table representing characteristics from several wings.

These wings were selected in order to assess the effect that geometry, wing area and AR have on the FWMAV's dynamics and performance. The wing 1 is considered the base model (Figure 3.7), since it was previously studied. Before construction, a Solidworks design has to be drawn for each wing, indicating measurements and angles (all of these designs can be found on Annex A). This procedure ensures the precision of every wing, preventing asymmetrical shapes.

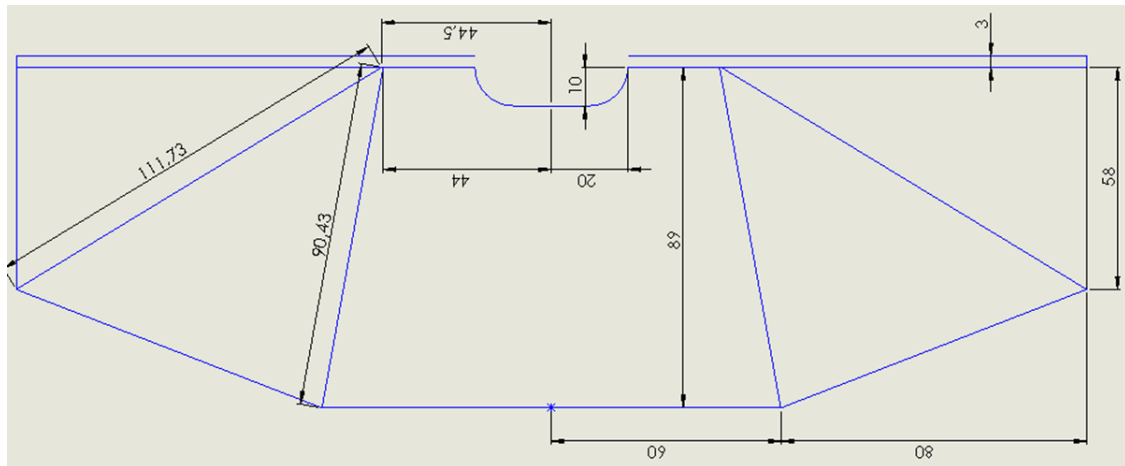


**Figure 3.7** – 140 mm wings with stiffener and section measurements (mm), not to scale (full dimensions in Annex A).

Then, the designs have to be printed in A4 and A3 size for the wing 2. Then, all the materials required for the wing assembly have to be gathered. The most important ones are carbon rods and mylar, since they make up almost 100% of the wing's weight. Mylar is a polyester film made from stretched polyethylene terephthalate (PET) and is used for its high tensile strength and lightness. They can be found with varied thickness, depending of their function. In the case of this project, three measures are in mind, namely 5, 10 and 15  $\mu\text{m}$  thick mylar. The thicker Mylar is, the stiffer the wing becomes. After looking into **Perçin (2015)** research where he studies and compares the effect that different mylar foil thickness have on lift generation, power consumed and thrust-to-power ratio, it is seen that 10  $\mu\text{m}$  thick mylar produces the highest peak force of all wings, thanks to a compromise between effective wing surface, angle of attack and wing camber, causing a greater wing deformation and an enhanced Clap-and-Peel effect. Conversely, the 5  $\mu\text{m}$  thick mylar is not able to produce the required lift, lacking to create a low-pressure region between the wings and therefore decreasing LEV circulation. Moreover, it is prone to tear up when working at full

throttle. With regard to the 15  $\mu\text{m}$  thick mylar, the additional weight causes more inertia and torque, overloading the flapping mechanism and increasing power consumption. The suction force due to wing area is also augmented, resulting on larger drag upon the flow separation. Therefore, the right choice tended for the 10  $\mu\text{m}$  thick mylar.

Carbon rods are responsible for providing structural rigidity and tension to the wings. As previously discussed, their diameter has influence on wing deformation. Therefore, 0.28mm carbon rod stiffeners are the ones to be installed. In regard to leading-edge carbon rods, they have to be resistant to withstand the flapping forces when changing direction. Thus, a semi-circular shape is preferred, since leading edge wings can maintain its shape, allowing the contact between them and promoting Clap-and-Peel effect. A small diameter can compromise the wing's structure, whilst a large one can increase torque and weight, so a compromise has to be found, resulting on the 1mm option.

After the main materials, the remainder ones responsible for cutting and gluing are chosen. Duct tape and polystyrene glue present the best option, since they are affordable and have enough strength to cope with flapping forces. However, a careful dose is needed when adding glue. If too much glue is applied, the weight will be increased and the remains can stick undesired components. A precision knife will also be needed to correctly cut mylar with the intended dimensions. In order to hold mylar in place while cutting it, at least four clamps are needed. A hard base also has to be acquired to protect the table against scratches. When cutting mylar, there has to be additional care, otherwise measures will get affected. If the wing is not stretched when cutting, it can result on a high tension when installed, therefore increasing motor workload and preventing wing deformation. Conversely, if tension is weak, aerodynamic forces will be less than desired (*Bruggeman, 2010, p. 80*).

The steps needed to fully construct a wing are presented in Annex C, which begin with the positioning of a wing design sheet between the hard base and a mylar sheet, securing them with four clamps. Then with a precision knife, the outer limit of the wing design is cut, firmly securing the sheet with the other hand. After obtaining a mylar wing, stiffeners and wing rods can be measured and cut.

The next stage is the glue process, in which carbon stiffeners are bonded onto mylar wings. For increased precision when positioning the rods, a pair of tweezers is used. Then, the rods connecting the wings to the flapping mechanism are glued to the leading edge, by carefully placing the wing rods about 3mm under the top limit of the wing to allow mylar to stick around them. After applying pressure to ensure a proper fit, a reinforcement of the extremities of the stiffeners, wing center and body clamp hole is made by cutting and gluing small pieces of duct tape. The production process has to be the same for the same wings in order to fully calculate and assess its performance.

### 3.1.3. Structural design of the tail

As explained on section 3.1, a tail is responsible for dynamic stability and control to the FWMAV. In order to simplify tail construction, the intended design is an inverted T-tail. The design itself tends to follow other projects like **Ferreira (2018)** or Delfly II, which have demonstrated superior control capabilities and ease of construction.

After analyzing **Ferreira (2018)** dissertation, there is a reference about a certain instability after applying rudder (cf. chapter 5.2.2 of Ferreira (2018)). This can be caused due to a lack of surface area needed to counteract the momentum caused by the rudder. Furthermore, its tail was made out of Styrofoam, which, while rigid, has considerable weight. By observing Figure 3.8, the rudder design was slightly changed, while maintaining the same horizontal stabilizer profile. This design was inspired on **Ferreira (2018)** FWMAV, where he adapted specific tail dimensions from **Caetano (2016, p. 27)**. The decision was to keep the design of the horizontal stabilizer, since it provided good stability and control. The trailing edge would be the same length of 135mm and to create an elliptical form, the chord length would be 55mm. With regard to the vertical stabilizer, **Ferreira (2018)** chose the measures in order to get a proportional tail. Therefore, the vertical stabilizer height had to be half of the horizontal length of the tail. With respect to the elevator, it is approximately one quarter of the total length of the surfaces, proportion chosen due to the low speeds of operation **Ferreira (2018)**. Moreover, two carbon rods of 136.47mm were placed diagonally to increase structural rigidity.

Conversely to the horizontal stabilizer, the vertical stabilizer had several issues already discussed before. Therefore, its area was increased to 105mm, creating an elliptical shape rudder with 50mm length. This modification should be able to increase stability and maneuverability. Lastly, a 60.19mm carbon rod was fitted diagonally to the rudder for rigidity purposes.

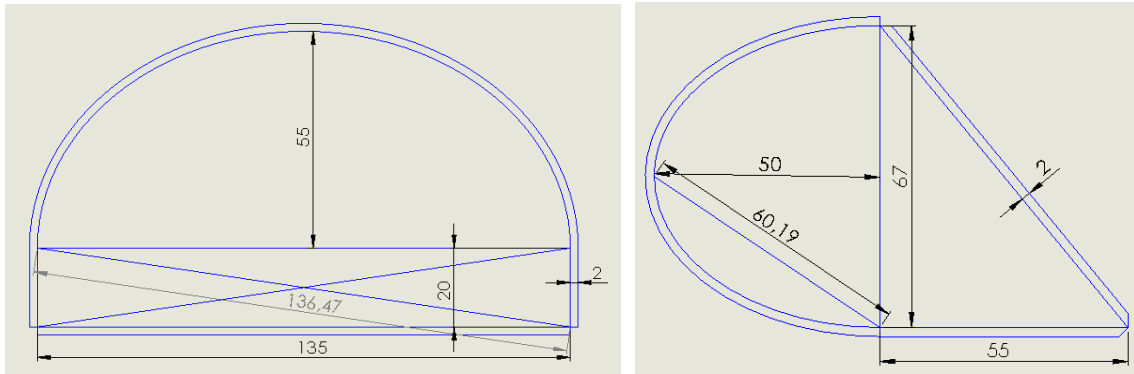


**Figure 3.8-** Tail design with stiffener and section measurements (mm) (not to scale): Top-Vertical stabilizer and Rudder; Down- Horizontal stabilizer and Elevator (Annex B).

Although more difficult to build, a mylar tail brings some advantages, like weight reduction and improved structural rigidity. With less weight, there is less momentum after applying rudder, which will considerably improve stability and, therefore, control. In Ferreira's design, the elevator and rudder were detached from the stabilizers, only placed together with duct tape. This freedom would create a vibratory movement induced by the wings, worsening dynamic stability.

Contrarily to Ferreira's Styrofoam tail, the control surfaces would be attached to the vertical and horizontal stabilizers, since they are made from the same exact mylar piece. Once wings and tail are made from the same components, the assembly process is also the same, with a difference that the duct tape reinforcement is made once the tail is fitted to the body, preventing vibrations and possible failures. The final aspect is shown on Figure 3.9, whose detailed assembly steps can be followed on Annex D.

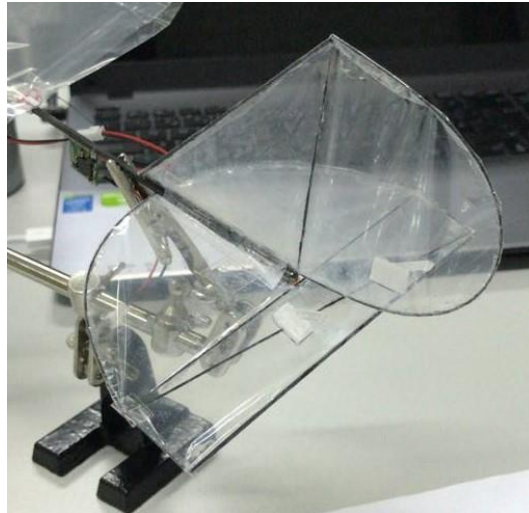


**Figure 3.9** - FWMAV Improved tail.

### 3.2. Electronics

The main electronics for the FWMAV consist in batteries, servos, a motor, an electronic speed controller (ESC), a receiver, an onboard-camera and a FPV receiver.

Beginning with batteries, three different capacities were available, all of them being lithium ion with 3.7V output: 100mah, 120mah and 150mah, whose weights are 3.3g, 4.5g and 6g respectively. The selection consists in the best compromise between capacity and weight. Thanks to the brushless motor, the lift capability would be significantly higher. Therefore, more payload is admitted, managing to install bigger batteries, increasing its endurance.

The motor is the element responsible for creating a rotational movement that powers the flapping mechanism. It plays a vital role in the lift generated and consequently, the maximum payload. Brushed motors are known for having a simple operation and an affordable price, being the most widely used in miniature applications. They are composed by a case that holds stator magnets with two poles opposite to one another. Inside it, the shaft is connected to a commutator and wire windings, that are energized when a pair of brushes make contact with the commutator. This electrical input generates a magnetic field, therefore moving the shaft. By constantly alternating the polarity of the magnetic field, a regular rotational movement is guaranteed.

Despite being more expensive, brushless units are capable of increasing power capacity as well as run time whilst maintaining its size. The principle consists in changing the stator electromagnet's poles by inverting the direction of the electric current, which will interact with the permanent rotor magnets, inducing a momentum. In order to charge up the electromagnets (coils), a computer (ESC) has to determine the position of the rotor to decide which ones have to be on. Brushless motor coils normally have 3 phases, depending on the current, they will attract one pole and repulse the other one. Only opposite coils are energized, enabling a larger amount of torque to be produced. Therefore, motor working will be more precise, as well as avoiding brushes to wear out. After considering the advantages and disadvantages, the decision was to acquire a brushless motor.

Actuators are responsible for powering the control surfaces, namely rudder and elevator. There are two types of actuators, linear and magnetic actuators. Linear actuators can produce a higher force, thus they are not susceptible to vibrations and disconnections. Conversely, magnetic actuators are considerably lighter (0.35g and 0.66g), nonetheless they have less power. Since a brushless motor will be able to provide an increased lift generation, more emphasis is given to reliability and better control inputs. However, due to acquisition problems, linear actuators couldn't be ordered. Therefore, magnetic actuators are the chosen ones to be installed.

A receiver is the FWMAV's motherboard, responsible for processing signals from the remote control and transmitting it to the motor and servos. The intended option would consist in a receiver with a built-in brushless ESC, saving unnecessary weight and wiring. Since there wasn't any available, a DelTangRx43d DMS2 compatible receiver was acquired (Figure 3.10). It has 4 channels, with a possibility for 3 actuators/servos to be connected. Furthermore, it has a weight of just 0.34g.



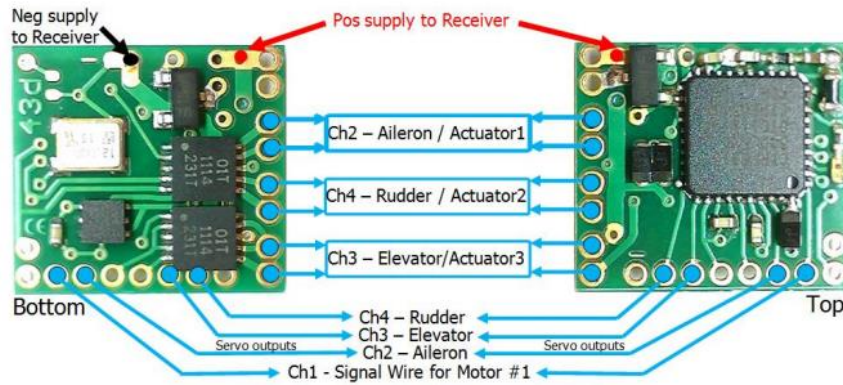


**Figure 3.10** – DelTangRx43d wiring for brushless motor output.

The electronic speed controller (ESC) in the component responsible for controlling the battery power output before going to the motor, and as explained before, ensures its smooth operation. In order to cope with a brushless motor, a 0.4g micro brushless ESC of 3A was acquired (Figure 3.11).

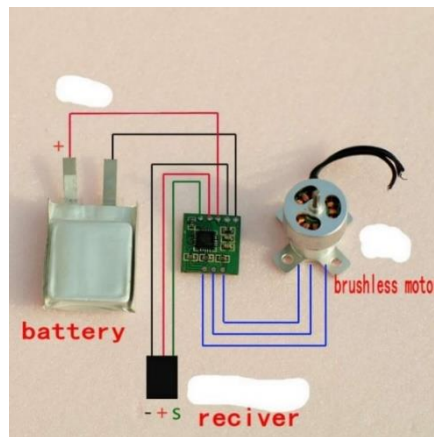


**Figure 3.11** – ESC electrical wiring.

### 3.3. Video streaming

A FPV system allows the control of the FWMAV indoors or outside our line of sight. Here, the video image from an onboard camera is transmitted by radio to a video display in the form of a screen or head goggles. Video transmission can be analog or digital. In analog transmission, the recorded images are sent to the receiver through a continuous signal, requiring no image compression or advanced processing, Therefore, latency is absent, which is the time difference

between the captured frame and the displayed frame. However, analog signal transmission on the same frequency can lead to a grainy image quality, jammed frequencies or even a total signal disruption. Despite these factors, analog FPV cameras are a compact and low-cost system. Digital transmission is made using a discrete signal, where an analog radio frequency is modulated with digital data, known as digital modulation. This separates the information going to each pixel rather than merging them together as is the case with analogue, resulting on a higher image quality. However, if using the same bandwidth as the analog system, the digital FPV system can either send a delayed image (high latency) or drop the video quality to decrease latency. Together with complexity comes a high cost, therefore the best option is an analog FPV system.

One big challenge about dealing with video transmission is interference and attenuation when flying indoors or near obstacles. There are several measures to solve the lack of signal according to **Bjørn Bergersen (2016)**, one of them is ensuring a reasonable front-end channel filtering of the video receiver, as well as the use of a directive ground antenna in order to minimize interference from other directions. FPV system antennas benefit additional signal strength when used with a narrow beam and high directional gain. On Figure 3.12 it is possible to observe the receiver signal process after image is transmitted. After some search, a reliable and affordable Fatshark Dominator V3 FPV system was found, thus enabling a screen connection (Figure 3.13).

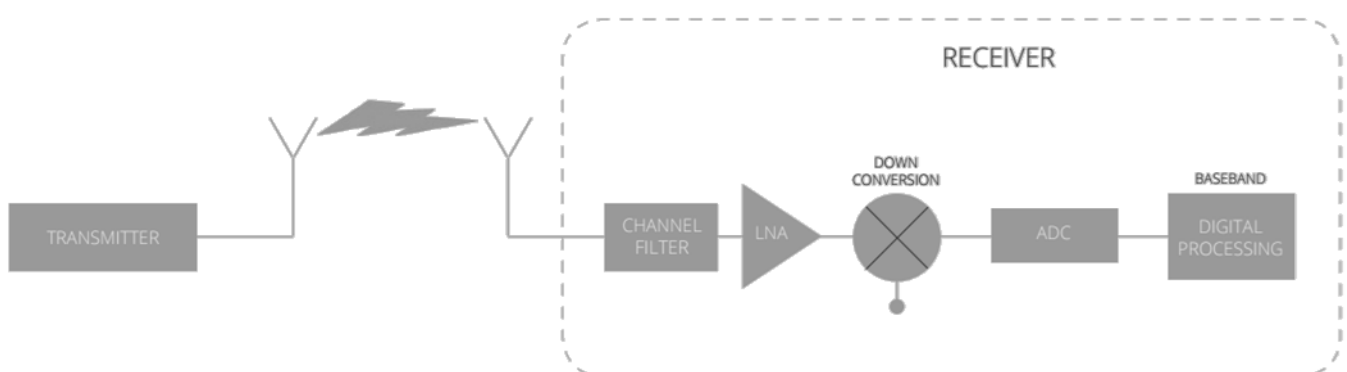


**Figure 3.12** – Receiver Signal Process.



**Figure 3.13** – Fatshark Dominator V3 FPV system.

The camera displayed on Figure 3.14 is a 5.8GHz 40ch FPV with a video transmitter already installed, weighing 3.6g. It was chosen based on its weight, since together with the battery, it is one of the heaviest pieces fitted on the FWMAV. Power consumption is also one factor that can limit FWMAV recording time, therefore the camera must be able to live stream with a low energy consumption. If using a 150mah battery, knowing that the camera has a power consumption of 380ma, the recording time would be approx. 23 min. Nonetheless, energy is mostly used by the motor, therefore camera operation will be severely limited. In order to power both the camera and the motor, an additional connector had to be added on the battery, as shown on Figure 3.15. Section 4.3 evaluates the influence of the FPV camera on flight time.



**Figure 3.14** - 5.8GHz 40ch FPV Camera.

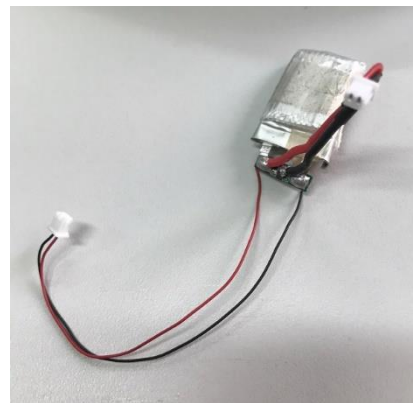


**Figure 3.15** - 150mah battery with additional connector.



## Chapter 4. Data analysis and comparison

In this chapter, different FWMAV wings will be assayed through several performance tests, viz., maximum lift generation, maximum payload, endurance, as well as highest flapping frequency. Based on these tests, wing efficiency will be determined and the influence of Aspect Ratio explained. Moreover, FWMAV's stability and control will be detailed.

#### 4.1. Lift generation and maximum payload

In this section, maximum lift capability of different wings will be addressed, by determining the maximum payload that the FWMAV will be able to carry during flight. For this test, flight time is not considered, since only hover capability will be tested. Furthermore, these tests have to be carried out identically, since there are slight variations on the air pressure and temperature over time.

Lift is quantified by loading small amounts of weight and applying maximum throttle until it struggles to maintain hover (Figure 4.1). Moreover, several batteries were used, in order to ensure the best performance. During this test, 150mah batteries were installed, since they are the ones with the most capacity. Contrarily to previous FWMAV developed at the PAF, hover capability was not affected by battery weight, hence confirming its improved performance. The objective is to carry out the same exact test with all five pairs of wings, in order to evaluate the one that has the best lift generation.

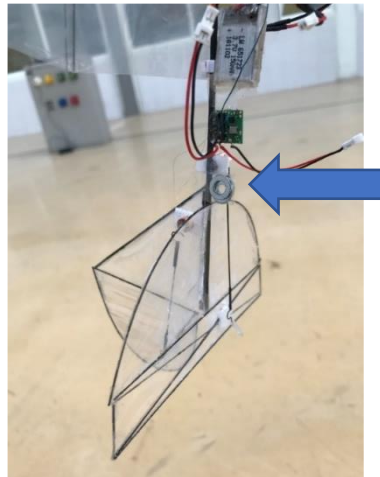


**Figure 4.1** – Maximum lift test, where small weights are added.

After doing the test, the results were clear. By observing Figure 4.2, the wing 3 had the most lift capability of 26.9g. Followed by the wing 1 (24g), the wing 2, (23.1g), the wing 5 (20.6g) and the least capable, the wing 4 (19.3g). The achieved results are in accord with **Bruggeman (2010)** and **Perçin (2015)** as presented in section 3.1.2.1, where they prove that bigger AR wings provide more lift. On section 4.4, the reason behind wing 1 providing more thrust is explained.

In regard to the wing 2, despite having more surface area, it provides less lift due to having more weight and consequently, more inertia. Moreover, the effective chord responsible for creating suction and enhancing LEV is smaller, resulting on a decrease of Clap-and-Peel effect. The results presented by the wing 5 were expected, once the lack of surface area near the outer edges prevents taking advantage of the increased tangential wing velocity near the wing tips. Lastly, the wing 4 had the worst results, once it has a smaller AR and wing area, diminishing the production of dynamic pressure caused by wing suction, therefore reducing LEV and circulation.

After subtracting the drone's weight from the lift generated, the maximum payload was then calculated. The results were also by the same order as the maximum lift: 7.6g (wing 3), 4.8g (wing 1), 3.5g (wing 2), 1.4g (wing 5) and 0.3g (wing 4). Each pair of wings has an influence on its final weight, which comprehends between 19g and 19.6g with the 150mah battery, already counting with the addition of the camera.

After cross-checking data with previous FWMAV researches, there is a 60% increase in lift generation if the same 140mm wing is considered; also, a 79.3% with the bigger AR wing. This increase is due to a more powerful brushless motor, however, 19.3% is caused by the different wing option.

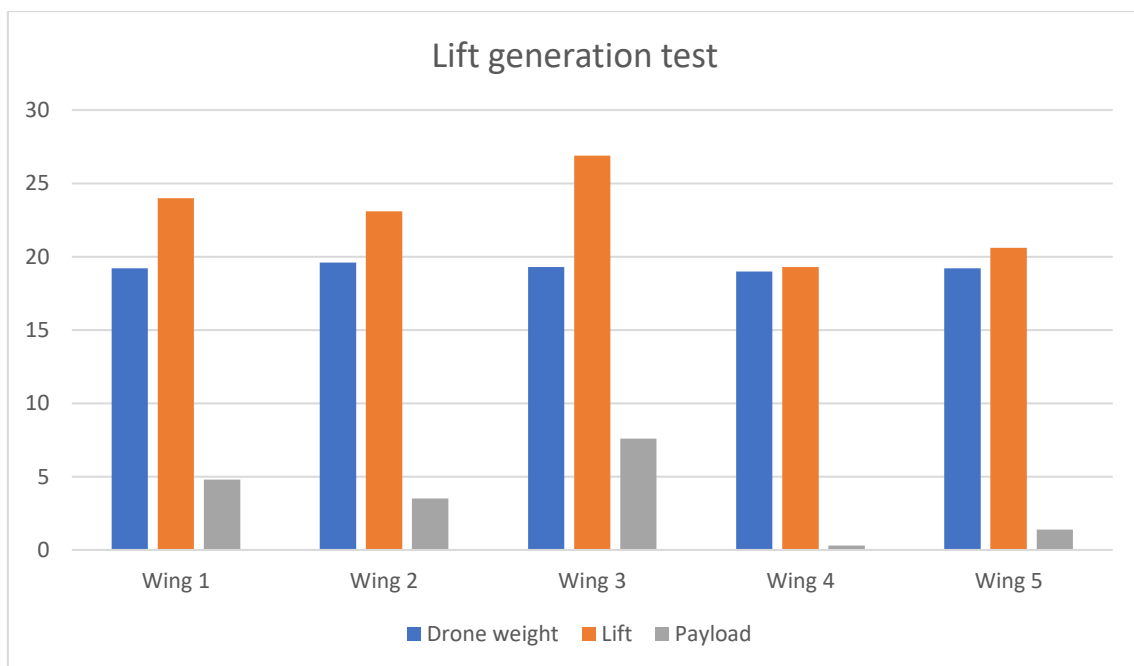


**Figure 4.2-** Lift generation test in order to calculate maximum lift capability (orange) and payload (grey), depending on drone's weight (blue).

## 4.2. Flapping frequency

Flapping frequency is a wing characteristic that depends on its area, form and materials. If the wing has less area, it moves a smaller amount of air, decreasing vacuum due to Clap-and-Peel and therefore having a higher flapping frequency. If the wing materials are heavy, they will have more inertia, hence lowering the flapping frequency due to increase in torque at the motor.

According to **Bruggeman (2010, 5.2.5, p.69)**, “In all the performance plots of the previous sections one can see that the relation between frequency and thrust and between frequency and power is quasi-linear.” By analyzing these graphics (Figure 4.3), we can conclude that considering the same wing, the higher the flapping frequency, the more thrust it will produce. Consequently, the power consumption will also increase. In order to produce the same amount of thrust, different wings have different flapping frequencies, therefore is beneficial to have a lower flapping frequency wing than enables hover with a lower power consumption.

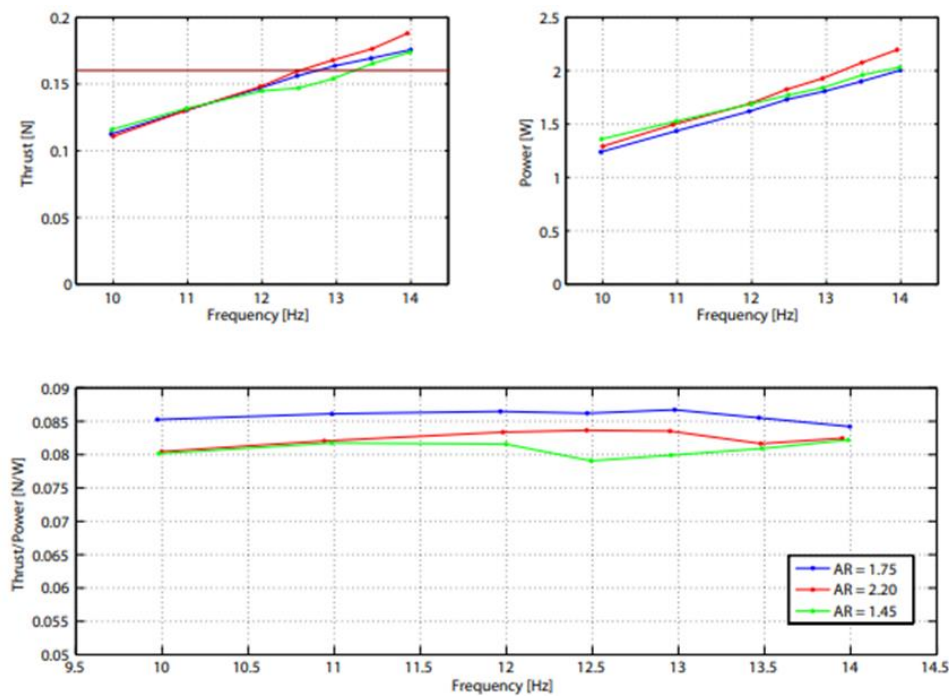
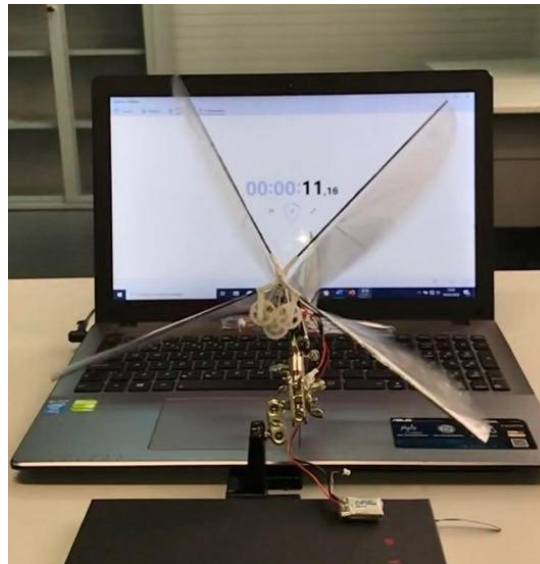


**Figure 4.3** – Bruggeman (2010, figure 5.2.2, p.69) graphics of different AR wings, relating flapping frequency, thrust and power.



To choose the best wings for the FWMAV, we have to take into account the highest flapping frequency it can achieve. If one given wing has to have a high flapping frequency just to enable hover, it will eventually decrease FWMAV flight time. Therefore, we have to find a wing that has a low flapping frequency and, moreover, it has to have a good lift capability, in order to ensure it doesn't struggle with the aerodynamic load.

To provide solid data about the maximum flapping frequency of the five pairs of wings produced, a 240 frame per second slow-motion video capture was used, where they perform at full throttle during one second (Figure 4.4). The number of flaps will then correspond to its frequency (Hz).<sup>1</sup>



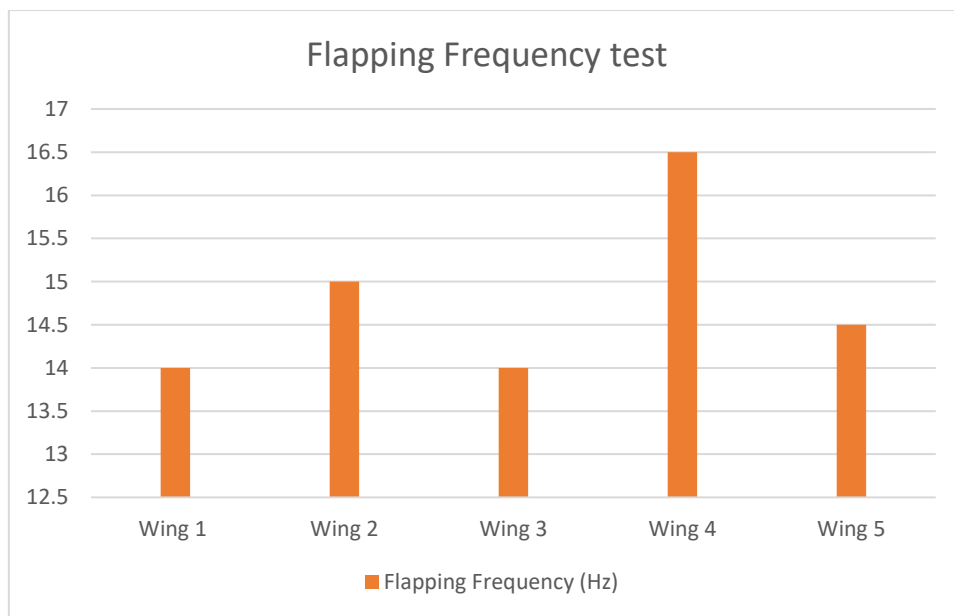
**Figure 4.4** – Flapping frequency test.

Figure 4.5 presents the maximum flapping frequency of each wing. Together with the results shown above, in Figure 4.2, wings 2, 4 and 5 are put out of interest, once they have a high maximum flapping frequency combined with a lower lift generation. Wings 4 and 5 have less span and wing area, displacing a smaller quantity of airflow, therefore having less inertia. This decreases torque produced by Clap-and-Peel, resulting on less lift generation. In order to produce

---

<sup>1</sup> The tests can be seen using this link below:  
[https://drive.google.com/drive/folders/1N5laGKJvXR0sPwxtO3C1DFIkdw\\_G0k66?usp=sharing](https://drive.google.com/drive/folders/1N5laGKJvXR0sPwxtO3C1DFIkdw_G0k66?usp=sharing)

enough thrust to hover, these wings would have to operate near the maximum flapping frequency, resulting on an increase of energy consumption. Despite being the one with the most surface area and therefore more inertia, the wing 2 had an unexpected high flapping frequency, possibly due to lack of foil tension and leading-edge rod damage from the previous test, halting production of vacuum and therefore having less airflow resistance. The others, namely the wings 1 and 3 are the ones that show the desired characteristics, since not only they have a low maximum flapping frequency of 14Hz due to a bigger wing area and airflow displacement, but also, they have the biggest lift generation of all. Hence, it proves the increased efficiency caused by the enhanced LEV and higher circulation. Regarding energy consumption, these wings would hover at a frequency lower than 14Hz, resulting on a lower power consumption.



**Figure 4.5** - Graphic illustrating the flapping frequency test, where the maximum flapping frequency (orange) of each wing is represented.

### 4.3. Endurance and efficiency

After choosing the two best wing options, other tests were carried out in order to determine the amount of time that the FWMAV could hover non-stop. The batteries, as well as the wings, are the parts that mostly influence this characteristic. By testing several possibilities, the objective of having the best

endurance time will be attained. The first two tests will focus on the different wings, while maintaining the same 150mah battery. They begin with the battery fully charged, and are finished when the FWMAV stops hovering.

After doing these tests, the wing 1 performed better than the wing 3. The first had an endurance of 9-10 minutes, while the second stopped hovering at 5-6 minutes. This concludes that although having more lift generation, the wing 3 requires more torque due to higher suction, thus increasing its power consumption and wing resistance, while decreasing FWMAV's endurance. Hence, wing 1 is the one that holds the best efficiency, since it consumes less energy for the same weight carried. Moreover, comparing to previous FWMAV, there is a flight time increase of 7 minutes, greatly on account of the brushless motor, which provides more torque and an efficient operation, as well as the flapping mechanism which allows for an increase in flapping efficiency.

Despite having more capacity, 150mah batteries are also 1,5g heavier than the 120mah ones. Therefore, in order to evaluate its weight influence, one more test was held with the 120mah battery, while maintaining the same 140mm wings. With the lighter battery, the FWMAV hovered for 5-6 minutes, presenting a worse performance when compared to the 150mah battery. Thus, despite the additional weight, the 150mah battery is able to ensure an improved endurance. These tests are carried while using the same battery setup, meaning that wing 3 can have more endurance than wing 1 if using a battery with more capacity, taking advantage of its bigger payload capacity. Conversely, wing 1 provides less payload to get a better battery. Nonetheless, if payload is fully used, the motor will produce maximum lift, increasing energy consumption while reducing flight time.

These flight times are measured with the FPV camera off, meaning that in a normal basis, the battery had to power both the camera and the motor. Therefore, motor consumption has to be measured in order to predict the flight time with the FPV camera on. In regard to the wing 1, if flight time is about 9-10 minutes, the motor consumption would comprehend between 900ma and 1000ma. Moreover, knowing that the camera consumes 380ma, flight time would be reduced to 6min30-7min. In respect to the wing 3, due to the higher drag, motor would

consume 1500 to 1800ma, resulting on an endurance of 4min11-4min47 with the camera on.

#### 4.4. Influence of the Aspect Ratio

As found in other studies, the AR has a considerable influence on the outcome of the results, e.g., **Bruggeman (2010, p.68)**: “One can see in the thrust-to-power ratio that the normal wing (140mm) gives the best performance. The wing with the higher AR however produces more thrust, especially at higher flapping frequencies. (...) The AR however has also influence on the Reynolds number, (...). This Re number has influence on the flow which will result in a higher thrust generation.”.

$$AR = \frac{R^2}{S} \quad (2)$$

This is the equation that permits the AR calculation, where R is wing span and S is the wing area. To increase the AR of a wing, its span can be increased; conversely, its area can be decreased. They can either be increased in the same proportion. In the case of this 160mm wing, the span was increased 15% and the area 13,3%, due to maintaining the chord length.

By using equation 2, it is possible to verify that the AR has increased about 15,2% from the 140mm to the 160mm wing:

$$AR_{140mm} = \frac{140^2}{11020} = 1.78,$$

$$AR_{160mm} = \frac{160^2}{12490} = 2.05$$

The reason behind the increase of lift generation lies on the Reynolds Number. As referred in section 2.1.1., this characteristic tends to decrease the relation between inertial forces and viscous forces for a given flapping frequency, hence enhancing the LEV. Moreover, the tangential wing velocity increases with the distance from the rotation axis. Equation 3 shows the relation between AR and Reynolds Number, where  $\varphi$  is the stroke angle, R is the wing length,  $\nu$  is the kinematic viscosity and  $n$  the flapping frequency.

$$Re = \frac{\varphi n R^2}{\nu AR} \quad (3)$$

By comparing vortex development between the high aspect ratio wing and the 140mm wing on Figures 4.6 and 4.7, it can be seen that the LEV are stronger and larger during the in-stroke and out-stroke. With regard to TEV, by analyzing both wings, it can be verified that they are shed at an earlier stage.

Circulation is also enhanced, thanks to a study carried by **M.A. Groen (2010)**: “For the improved wing, the LEV circulation at the end of the instroke is  $260 \text{ cm}^2/\text{s}$  while for the high aspect ratio wing the circulation found for the investigated region is  $452 \text{ cm}^2/\text{s}$ . This is a clear increase in circulation of about 70%. For the LEV at the end of the out-stroke the circulation is calculated in the same manner. The value found for the circulation is overall higher, but still there is a clear increase in circulation for the high aspect ratio wing:  $546 \text{ cm}^2/\text{s}$  for the 140mm wing and  $754 \text{ cm}^2/\text{s}$  for the high aspect ratio wing (an increase of about 40%).” (p.56, section 6.4.3).

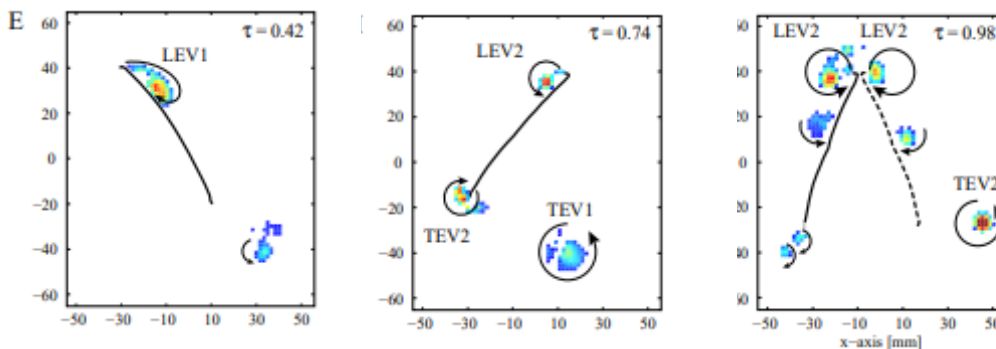


**Figure 4.6** - Swirling strength at the end of the out-stroke (E), halfway during the in-stroke (I) and at the end of the in-stroke (L) for the 140mm wing. Showing leading edge vortices (LEV) and trailing edge vortices (TEV). (M.A. Groen, 2010).

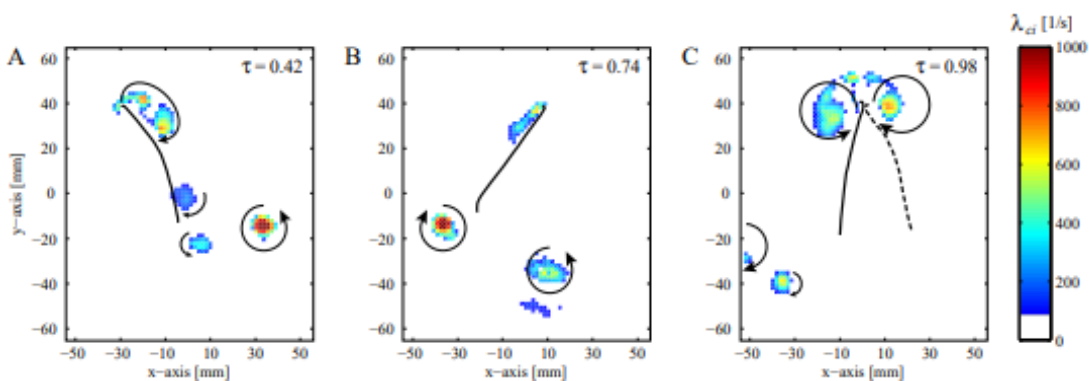


**Figure 4.7** - Swirling strength at the end of the out-stroke (A), halfway during the in-stroke (B) and at the end of the in-stroke (C) for the high aspect ratio wing (M.A. Groen, 2010).

Nevertheless, this change on the airflow that creates a higher thrust generation is not only due to Reynolds Number, as **M.A. Groen (2010, p.55, chapter 6.4)** on *PIV measurements on the hovering DeIFly* explains: “Other similarity parameters like the Strouhal number and Rossby number will also play a role, but an important effect is the aero-elastic effect. Changing the wing size will change the inflight wing deformation and hence create a different air flow.”. I.e., during stroke reversals, the leading edge moves to the opposite direction before the wing surface, resulting on a wing deformation. Aero-elastic effect is triggered by the component inertia, meaning that the bigger the wing size, the more inertia is created, following an increased wing displacement. However, wing deformation at high flapping frequencies also cause a decrease on the geometric angle of attack during translation as well as an increased heaving motion, weakening LEV and consequently losing efficiency.

#### 4.5. Stability and Control

Stability and control are essential for video recording and flight, therefore the FWMAV must be optimized to operate according to a flight envelope. These adjustments would not only prevent instability, but a possible total loss of the FWMAV. Therefore, the Center of Gravity (COG) must be carefully measured to achieve stability during hover, forward/backward flight and when applying surface controls. Previous studies, e.g. **Caetano (2016), Ferreira (2018), et.al.**, detailed different component configurations to enhance maneuverability or reduce oscillations. This made by shifting the COG in relation to the aerodynamic uplifting force. If distance is increased, the FWMAV becomes more stable after control inputs, nonetheless tail inputs become less effective. Whereas if decreased, the FWMAV becomes more responsive, yet more unstable and hard to control.

Given the number of components placed throughout the body rod, there was no space for large setups. The heaviest components, namely the camera and the battery weighting 3.6g and 6.0g respectively, were fitted in a central position, promoting a balance between stability and control effectiveness. Due to this weight difference, the camera was glued closer to the front, since it is a lighter component, reducing unstable contributions. Moreover, by positioning the

camera centered to the FWMAV, image capture would be more stabilized. Regarding the lighter components, namely the ESC and the receiver, they were glued to the extremities, since they create less momentum forces. The ESC had to be linked to the motor, therefore it was placed at the front. Whereas the receiver transmits electrical signals to the magnetic actuators placed at the back, so it had to be glued next to the tail. On Figure 4.8 it is possible to visualize the component setup.

After flight tests were carried, the FWMAV presented no signs of oscillations even after tail surface controls were applied. Moreover, throttle variation had no impact on stability. However, a lack of control was noticed, greatly on account of the low power magnetic actuators. These components did not provide enough force to achieve a desired trajectory or to correct a certain movement. If using no tail controls, the FWMAV would perform an anti-clockwise trajectory at a slow forward flight. To counteract it, a right/backward input was always necessary to achieve a straight flight, resulting on a constant power consumption from the actuators. With regard to forward/backward movement, the elevator had to be carefully applied in order to provide a forward momentum. If too much was applied the FWMAV would lower its nose, achieving high speeds and becoming uncontrollable. Despite providing a good forward effectivity, the elevator couldn't provide a backward movement due to the lack of power of the magnetic actuators.

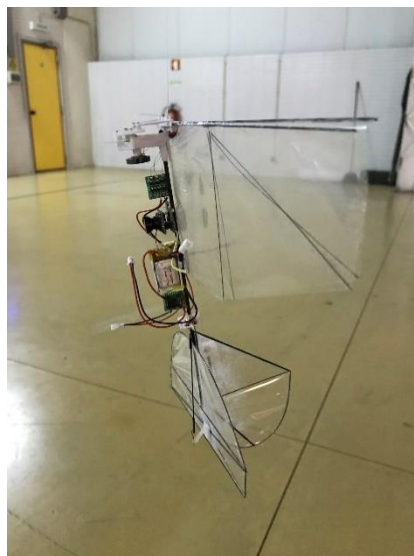


**Figure 4.8-** FWMAV component setup.





## Chapter 5. Conclusions and Recommendations

---

This chapter presents an outline of the FWMAV development, referring the major challenges throughout the stages, the achieved results and its conclusions, as well as establishing further development for the next researches.

In recent years, thanks to technological improvements and researches, several projects were carried out in order to comprehend the complex flapping wing dynamics and aerodynamics, thereby enabling the development of the very first nature inspired Flapping Wing Micro Aerial Vehicles (FWMAV). Their aerodynamic behavior however, is far different from the fixed wing and rotary-winged aircraft, affecting the way lift is generated.

At the beginning of this dissertation, an introductory question was stated “How to develop a flapping wing micro air vehicle with live streaming capabilities?”.

In order to hold some fundamentals, previous researches (e.g. the ones made by **Bruggeman (2010)**, **M.A. Groen (2010)**, **et al.**) were analyzed, where they measured the influence of flapping wing characteristics like flapping frequency, Clap-and-Peel, as well as different wing designs and sizes. Since there were no researches made in regard to these topics in the PAF, the decision made led to a study in order to improve the FWMAV wings, by evaluating the effect that geometry, wing area and AR have on the FWMAV’s dynamics and performance. Therefore, five different wings were designed and built, hence drawing useful data about lift generation, flapping frequency, endurance and wing efficiency. With regard to designs, the choices tended for: 1- a standard 140mm wing, 2- a 15% proportionally bigger than the 140mm wing, 3- a larger aspect ratio wing with a span of 160mm, 4- a less span 119mm and 5- an elliptical 140mm wing. Since other researches only analyzed the influence of AR by decreasing wing chord, the objective was to evaluate wing performance with a higher AR, hence increasing wing span whilst keeping chord length. For the wing’s structure, since stress and dynamic forces are high, it means that the material is prone to wear over time, i.e., the choice tended for a 10  $\mu\text{m}$  thick mylar. Despite creating more inertia due to higher weight, over the long term is able to maintain its lift properties, in contrast to a thinner one. By adopting this approach, it implies that the stiffeners have to be thinner, in order to enhance Clap-and-Peel. Therefore, their measure was about 0.28mm. The leading-edge rods were also semi-circular, allowing both wings to touch at the end of the in-stroke.

Thereafter, tail design was inspired on Ferreira (2018) FWMAV, while suffering structural changes, by modifying the vertical stabilizer design in order to increase surface area, thus increasing stabilization and control. Mylar was then opted

instead of Styrofoam, since the tail is 55.6% lighter and can ensure an improved structural rigidity.

Concerning FWMAV electronics, the objective was to apply for better material like powerful yet lighter linear actuators, or even a receiver with built-in brushless ESC. However, bureaucratic constraints meant that the assembly had to be made with the existent material. Nonetheless, some upgrades were made, fitting a brushless motor and Bruggeman's improved flapping mechanism, which provided a good power transmission and low energy loss. Due to an enhanced payload, 120mah and 150mah batteries were used, increasing operational flight time. The 5.8GHz 40ch FPV analog camera was chosen for its low latency transmission and low cost.

## 5.1. Conclusions

The created FWMAV met the intended targets, being able to provide a better performance, hence making a step forward in regard to flapping flight research for the PAF. Its specifications developed into a 19-19.5g FWMAV, composed by a bi-plane configuration, 10  $\mu$ m thick mylar wings, 1mm semi-circular leading-edge carbon rods and 0.28mm carbon rod stiffeners, ensuring Clap-and-Peel effect. The body structure consists on a 4mm thick carbon rod, large enough to support all the electronics glued under it. The tail was re-designed, replacing Styrofoam for Mylar, resulting in a weight saving of 0.4g, strengthening its mechanism and improving flight stability after control inputs.

Electronics were the components that ought to be improved, in order to get better performance, namely DelTang's RX43d receiver and the electromagnetic actuators. The receiver should have a built-in brushless esc, in order to save weight and prevent electrical failures due to cable disconnections. Regarding the actuators, they showed a poor induced force, limiting the tail's surface operation and impacting control effectiveness. Moreover, the constant usage severely drained the battery, thus decreasing flight time. The best choice tended for linear actuators, enabling to create a more controlled movement, moreover, the force would be increased thanks to small mechanical motors. The 5.8G 40ch FPV

camera displayed a good resolution, low latency streaming and recording smoothness thanks to the X-wing stability.

With regard to the lift generation and maximum payload test, data acquired revealed that wing 1 was the wing with the best performance, capable of generating 26.9g of thrust, therefore being 79.3% higher than previous prototypes. This is explained by the bigger AR, causing a decrease on Reynolds Number and enhancing LEV and circulation. These phenomena, together with the Aero-elastic effect, can increase wing vacuum and Clap-and-Peel. Wing 3 also presented the best payload capability of 7.6g, enabling to install a bigger battery.

In regard to the flapping frequency test, wing 1 and 3 presented the lowest maximum flapping frequency of 14 Hz, while wing 4 had the highest one. Low flapping frequency is due to a bigger wing area and airflow displacement, creating more vacuum between the wings and resulting on a higher torque resistance. Conversely, wing 4 has a less wing area and AR, displacing a smaller airflow and therefore having less torque resistance, being able to achieve higher flapping frequencies. To maintain hover, wing 4 has to perform near full throttle, resulting on a higher energy consumption. When comparing lift generation with maximum flapping frequency, wings 1 and 3 are the best performers, once they provide the biggest lift generation at the lowest flapping frequencies. Hence, it proves the increased efficiency caused by the enhanced LEV and higher circulation, allowing the FWMAV to maintain hover with a low power consumption.

After the endurance test, wing 1 presented the best results, achieving a 9-10 minute flight, exceeding prior versions by 7 minutes. Hence, it is the most efficient wing, since it consumes less energy while carrying the same weight. This time was set while using 150mah batteries, that despite its additional weight, their increased capacity enables a greater flight time by 4 minutes, in comparison with the 120mah. With this flight time, motor consumption would comprehend between 900ma and 1000ma. Moreover, considering camera consumption of 380ma, flight time would be reduced to 6min30-7min. However, both wings could achieve a higher flight time if using a bigger battery, due to higher payload capacity.

With regard to stability, placing the heavier components at the center and the lighter ones at the extremities proved to be beneficial, preventing undesired

oscillations while enhancing maneuverability. However, a lack of control was revealed on account of the low power magnetic actuators, not providing enough force to achieve a desired trajectory or to correct a certain movement. Moreover, if using no tail controls, the FWMAV would perform an anti-clockwise trajectory at a slow forward flight, always requiring a right/backward input to achieve a straight flight, resulting on a constant power consumption from the actuators.

## 5.2. Recommendations and Future Work

Some of the improvements needed in order to further increase the FWMAV capabilities are the acquisition of better electronics, namely a receiver with an integrated brushless esc in order to save weight and prevent electrical failures (a frequent problem during flight tests), as well as linear actuators to get more movement precision and force application. Since batteries wear out at a fast pace, energy available will be decreased, therefore they should also be upgraded for new ones with more capacity. Additionally, more tests have to be made concerning livestream capabilities, namely maximum flight time while recording, maximum range and flight outside line of sight. With regard to endurance, tests with wing 1 and 3 have to be made while using more capable batteries, taking advantage of their payload to increase flight time.

The broadening and research about the identification of aerodynamic force components, as well as wing flexibility effects in Clap-and-Fling should also be undertaken. This could be achieved by testing different geometric wings with different stiffener positions. Moreover, by integrating sensors and gyroscopes on the FWMAV body, auto-pilot would be a beneficial characteristic, since it could enhance the operation spectrum on the battlefield without the need of human action.

Bringing to a conclusion, these flapping vehicles are constantly undergoing researches, developments and enhancements, making them an interesting subject for further dissertations. Since these studies were carried out in recent years, there is still a lot to seize and discover.



# Bibliography

---

- Aliexpress. ESC electrical wiring. Retrieved from Aliexpress:  
<https://pt.aliexpress.com/item/32821319020.html?spm=a2g0s.9042311.0.0.3760b90aQBzYyL> (accessed on 2020, January 15)
- Bjørn Bergersen (2016), Specialist Development Engineer, Data Respons:  
<https://www.datarespons.com/drones-wireless-video/>
- Bruggeman, B. (2010). Improving flight performance of DelFly II in hover by improving wing design and driving mechanism:  
<http://www.delfly.nl/publications/MSc-Bruggeman.pdf>
- Caetano, J. V. (2015a). Caetano, J. V., Armanini, S. F., de Visser, C. C., de Croon, G. C. H. E., and Mulder, M. Data-Informed Quasi-Steady Aerodynamic Model of a Clap-and-Fling Flapping Wing MAV. International Conference on Unmanned Intelligent Systems. Bali, Indonesia.
- Caetano, J. V. (2016). Model Identification of a Flapping Wing Micro Aerial Vehicle. TUDelft.
- Delft University of Technology. The DelFly Project. Retrieved from Micro Air Vehicles Laboratory: <http://www.delfly.nl> on (2017, October 20)
- Dickinson, M. H., & Götz, K. G. (1993). Unsteady aerodynamic performance of model wings at low Reynolds numbers. *J. Exp. Biol.*, 174, 45-64.
- Dickinson, M., Lehmann, F., & Sane, S. (1999). Wing Rotation and the Aerodynamic Basis of Insect Flight. *Science*, 284(5422):1954–1960.
- Doswell III, C. (2000, November 27). A Primer on Vorticity for Application in Supercells and Tornadoes. Retrieved from Cooperative Institute for Mesoscale Meteorological Studies:  
[http://www.cimms.ou.edu/~doswell/vorticity/vorticity\\_primer.html](http://www.cimms.ou.edu/~doswell/vorticity/vorticity_primer.html)
- Dudley, R. (2000). *The Biomechanics of Insect Flight: Form, Function, Evolution*. Princeton University Press. ISBN: 9780691094915.
- Ellington, C. P. (1984a). The aerodynamics of hovering insect flight. IV. Aerodynamic mechanisms. *Philosophical Transactions of the Royal Society of London Series B, Biological Sciences* (1934-1990),

- 305(1122):79–113, DOI 10.1098/rstb.1984.0052.
- Ellington, C. P. (1984b). The aerodynamics of hovering insect flight II. Morphological Parameters. *Philosophical Transactions of the Royal Society of London. Series B, Biological Sciences*, 305(1122):17–40.
- Ellington, C., van den Berg, C., & Willmott, A. (1996). Leading-edge vortices in insect flight. *Nature*, 384(19/26):626–630.
- Fatshark Dominator V3 FPV system. Retrieved from Fatshark: <https://www.fatshark.com/product/dominator-v3-fpv-headset-goggles/> (accessed on 2019, December 10)
- Ferreira, L. (2018). Development of a Flapping Wing Micro Aerial Vehicle.
- Groen, M. (2010). PIV and force measurements on the flapping-wing MAV DelFly II. In MS thesis (Issue December 2010): <http://www.delfly.nl/publications/MSc-Groen.pdf>
- Holton, J. R. (1979). Edited by. iv. [https://doi.org/10.1016/s0074-6142\(08\)60513-6](https://doi.org/10.1016/s0074-6142(08)60513-6)
- Kramer VM (1932) Die zunahme des maximalauftriebes von tragflugeln bei plotzlicher anstellwinkelvergrosserung (boeneffekt). *Z Flugtech Motorluftschiff* 23:185–189
- Lapa, A. (1928). *Em Aviação Portuguesa*. Lisbon: Libanio da Silva.
- Lehmann, F. O., & Pick, S. (2007). The aerodynamic benefit of wing-wing interaction depends on stroke trajectory in flapping insect wings. *Journal of Experimental Biology*, 210(8), 1362–1377: <https://doi.org/10.1242/jeb.02746>
- Leonardo da Vinci's wing designs for proposed flying machine. Retrieved from Fircroft: <https://www.fircroft.com/blogs/celebrating-leonardo-da-vinci-the-worlds-greatest-engineer-91222165748> (accessed on 2019, November 14)
- Lighthill, M. J. (1973). On the weis-fogh mechanism of lift generation. *Journal of Fluid Mechanics*, 60:1–17.
- Marden, J. H. (1987). Maximum lift production during takeoff in flying animals. *The Journal of Experimental Biology*, 130:235–238.
- Micronwings. DTRx43d Receiver Unit for Servos. Retrieved from Micronwings: <https://micronwings.com/Products/DelTangRx43d/index.shtml> (accessed on 2019, December 20)
- Micronwings. DTRx43d Instructions. Retrieved from Micronwings:



- <https://micronwings.com/Products/DeITangRx43d/DTRx43d%20Instructions.pdf>  
(accessed on 2019, December 20)
- Micronwings. Micronwings. Retrieved from <http://www.micronwings.com>  
(accessed on 2019, November 20)
- Miller, L. A. and Peskin, C. S. (2005). A computational fluid dynamics of 'clap and fling' in the smallest insects. *Journal of Experimental Biology*, 208(2):195–212.
- Nabawy, M. R. A., & Crowther, W. J. (2017). The role of the leading edge vortex in lift augmentation of steadily revolving wings: A change in perspective. *Journal of the Royal Society Interface*, 14(132):  
<https://doi.org/10.1098/rsif.2017.0159>
- Norberg, R. Å. (1975). *Swimming and Flying in Nature: Volume 2*, chapter Hovering Flight of the Dragonfly *Aeschna Juncea* L., Kinematics and Aerodynamics, pages 763–781. Springer US, Boston, MA.
- Object moving through airflow. The airline Pilots. Retrieved from  
<https://www.theairlinepilots.com/forum/viewtopic.php?f=26&t=365>  
(accessed on 2019, December 20)
- Parker, D. (2001, September). ENVI 2210 - Atmosphere and Ocean Dynamics. Retrieved from School of the Environment, University of Leeds:  
<https://web.archive.org/web/20040406075109/http://www.env.leeds.ac.uk:80/envi2210/>
- Perçin, M. (2015). Aerodynamic Mechanisms of Flapping Flight. TUDelft:  
<https://repository.tudelft.nl/islandora/object/uuid%3A4d535d87-d11e-4916-9143-5e6762c56152>
- Phillips, N., & Knowles, K. (2010). Reynolds number and stroke amplitude effects on the leading-edge vortex on an insect-like flapping wing. *International Powered Lift Conference 2010*, September 2010, 365–374.
- Polhamus, E. C. (1971). Predictions of vortex-lift characteristics by a leading-edge suction analogy. *Journal of Aircraft*, 8(4):193–199
- Receiver signal process. Retrieved from Data Respons:  
<https://www.datarespons.com/wp-content/uploads/2016/03/mimo-with-base-band-weighting.png> (accessed on 2019, February 14)
- Sane, S., & Dickinson, M. (2001). The control of flight force by a flapping wing: lift and drag production. *The Journal of Experimental Biology*, 204(Pt

15):2607–26.

- Sane, S. P. (2003). The aerodynamics of insect flight. *Journal of Experimental Biology*, 206(23):4191–4208.
- Sane, S., & Dickinson, M. (2002). The aerodynamic effects of wing rotation and a revised quasi-steady model of flapping flight. *The Journal of Experimental Biology*, 205(Pt8):1087-96.
- Sedov, L. I. (1965). Two-Dimensional Problems in Hydrodynamics and Aerodynamics (ed. C. Chu, H. Cohen and B. Seckler), pp. 20-30. New York: Interscience Publishers.
- Wagner, H. (1925). *Über die Entstehung des dynamischen Auftriebes von Tragflügeln*. VDI-Verl.
- Weis-Fogh, T. (1972). Energetics of hovering flight in hummingbirds and in drosophila. *Journal of Experimental Biology*, 56:79–104.
- Weis-Fogh, T. (1973). Quick estimates of flight fitness in hovering animals, including novel mechanisms for lift production. *Journal of Experimental Biology*, 59:169–230.
- Weis-Fogh, T. (1975). *Flapping flight and power in birds and insects, conventional and novel mechanisms*, volume 2. Springer US.

# Annexes

---

Annex A – Wing Designs.....	1
Annex B – Tail designs.....	1
Annex C – Wing Detailed Construction Process.....	1
Annex D – Tail Detailed Construction Process.....	1
Annex E – Material Mass and source.....	1

## Annex A – Wing Designs

**Figure A-1** – 140mm wings with stiffener and section measurements (mm), not to scale.

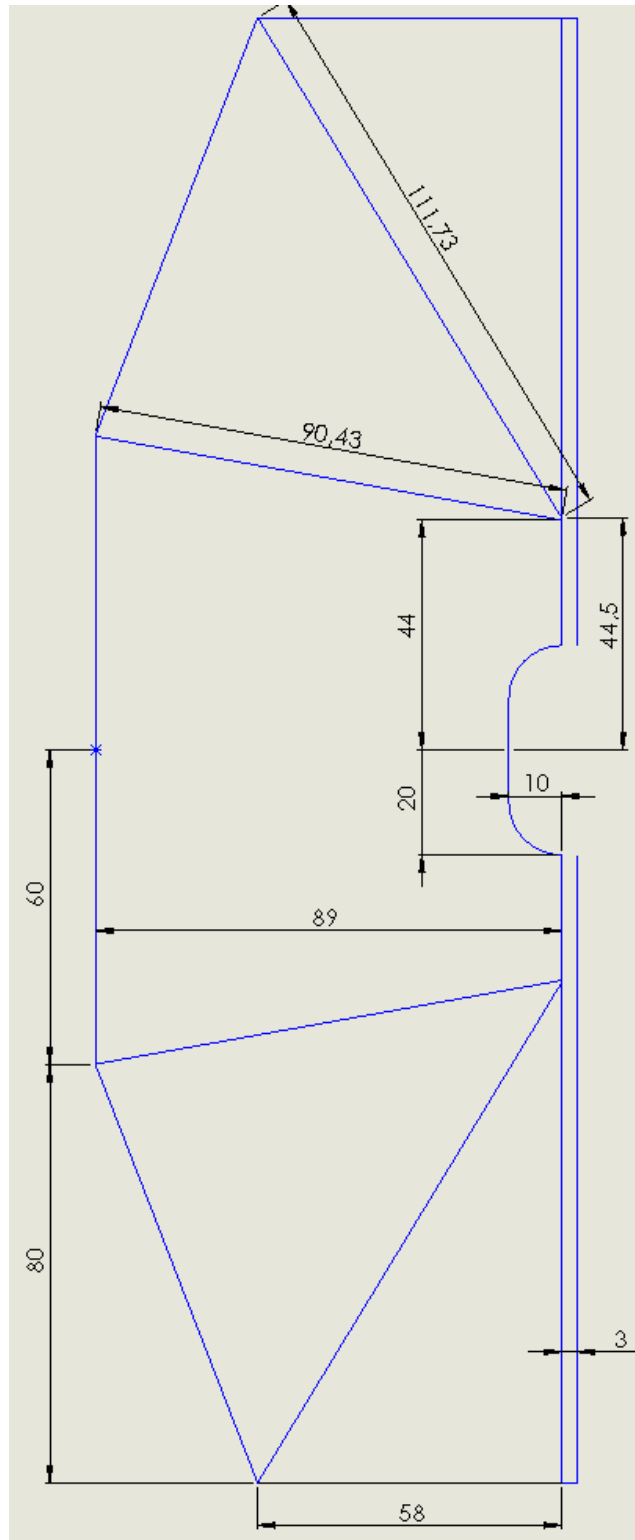


**Figure A-2** – 160mm with more AR wings with stiffener and section measurements (mm), not to scale.

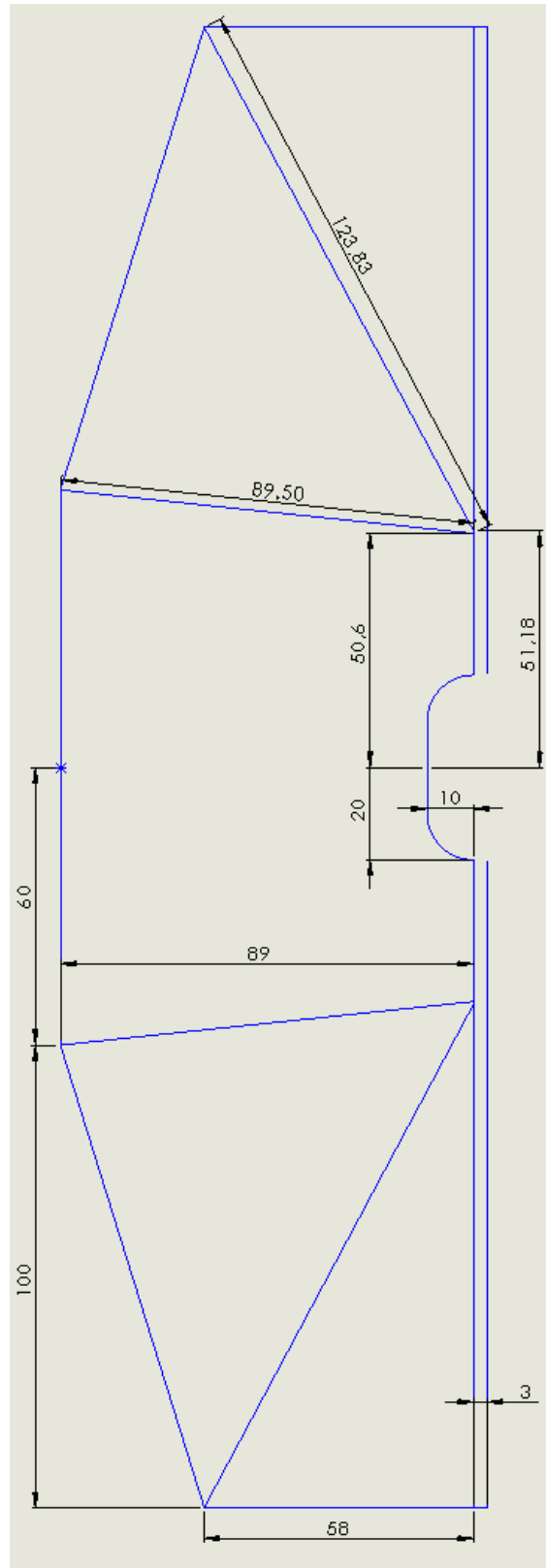


**Figure A-3** – 15% bigger than 140mm wings with stiffener and section measurements (mm), not to scale.

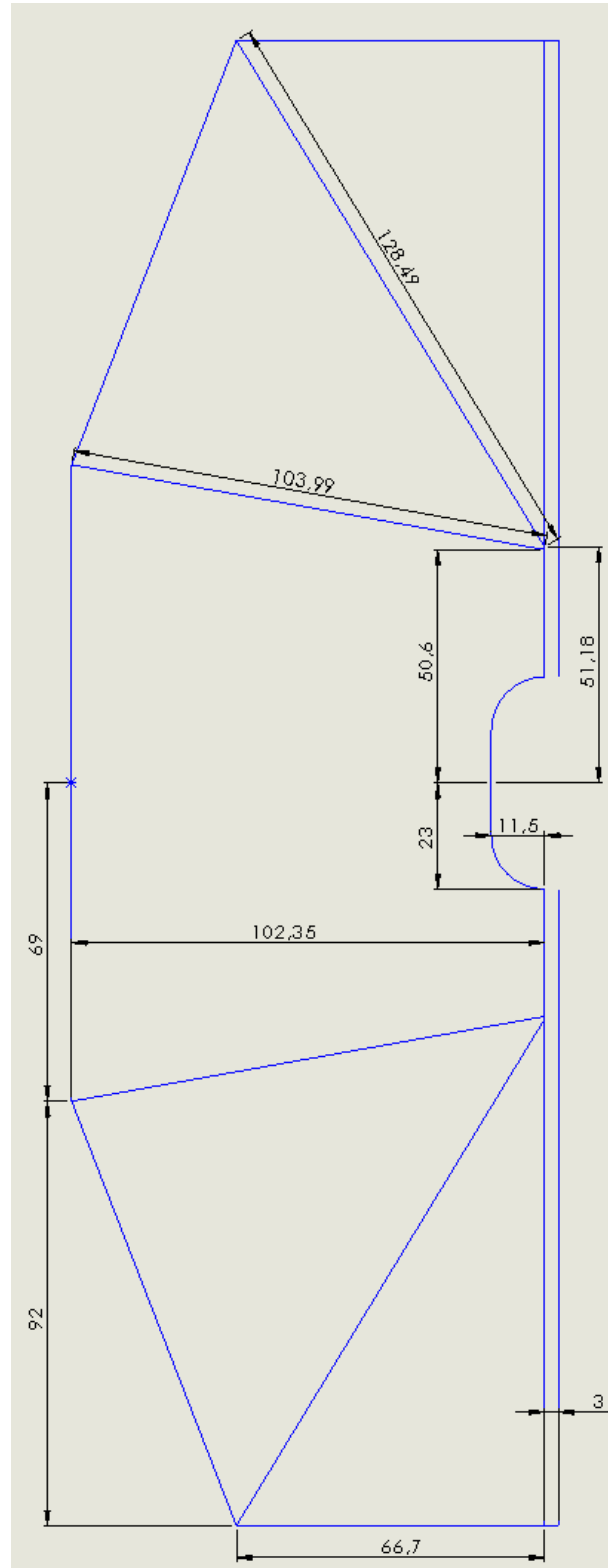


**Figure A-4** –119mm with more chord wings with stiffener and section measurements (mm), not to scale.

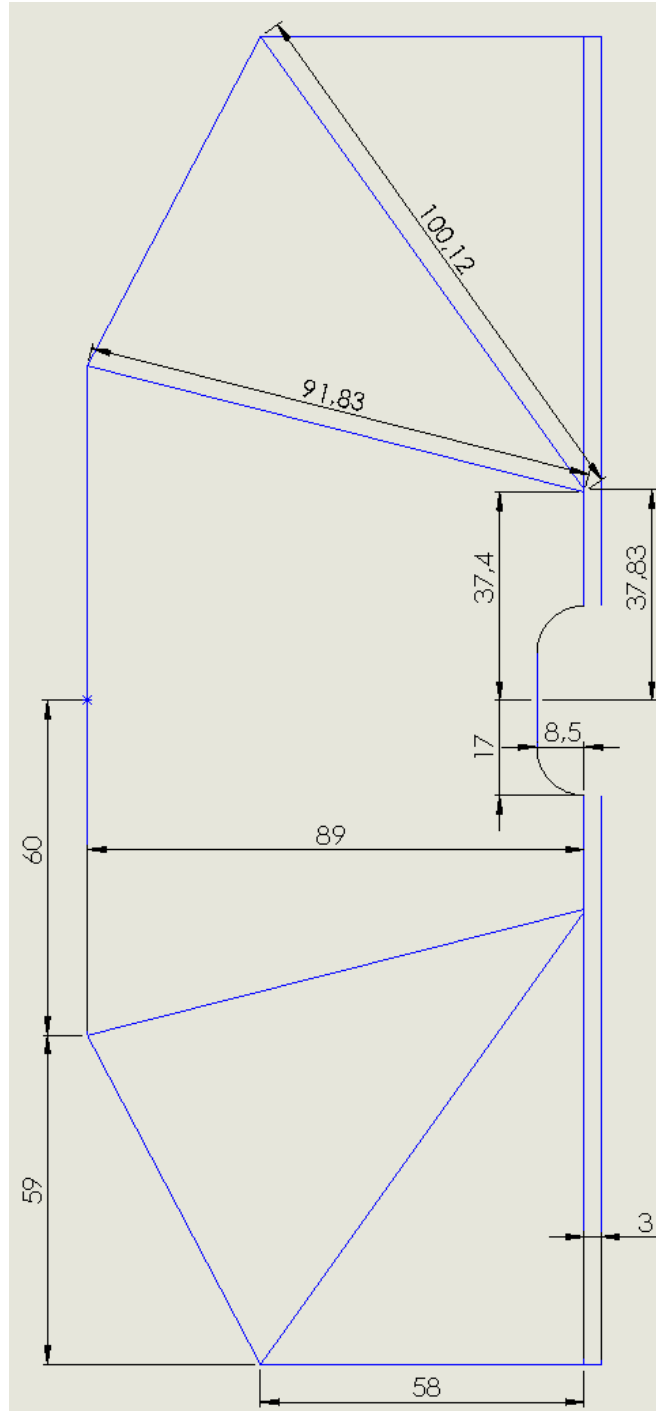
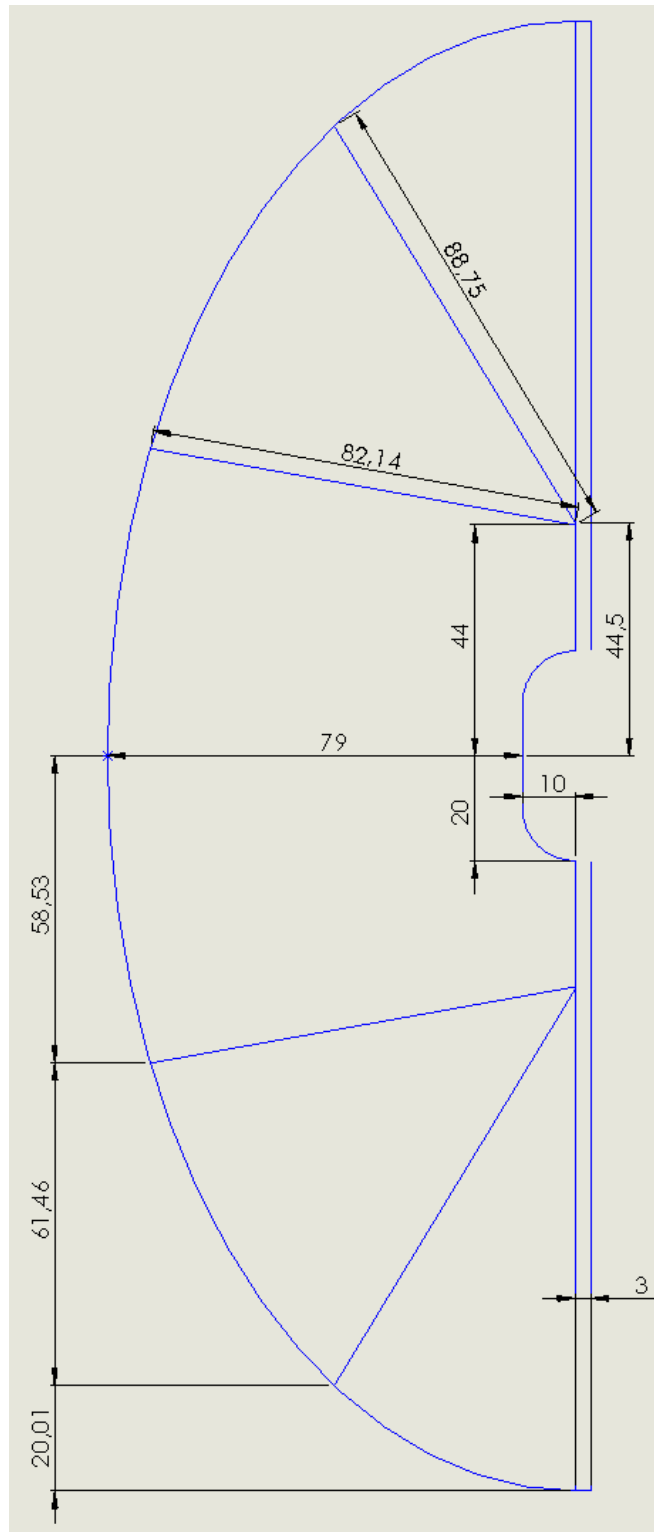


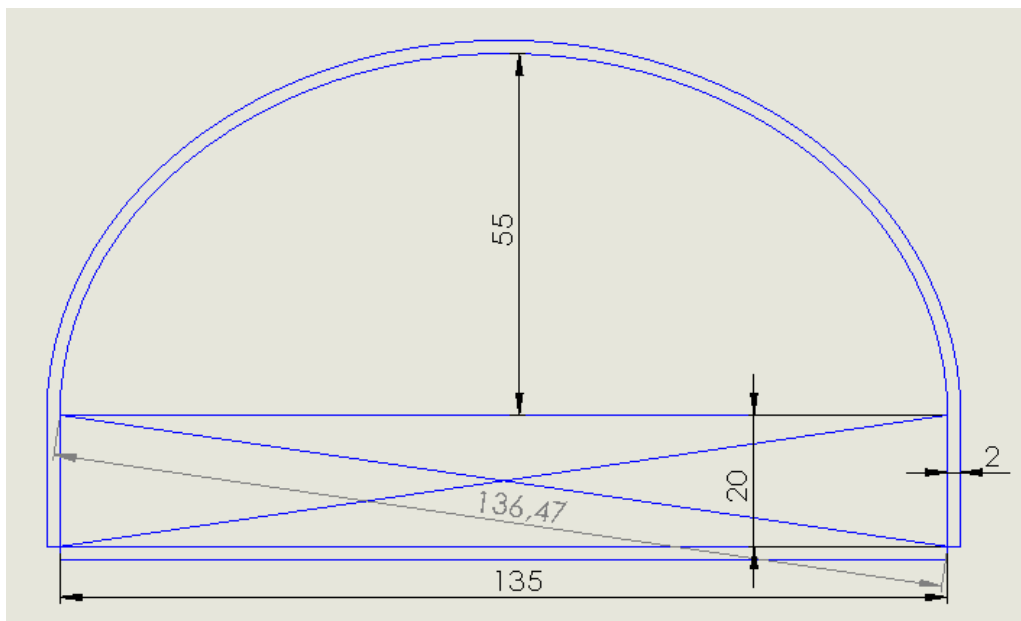
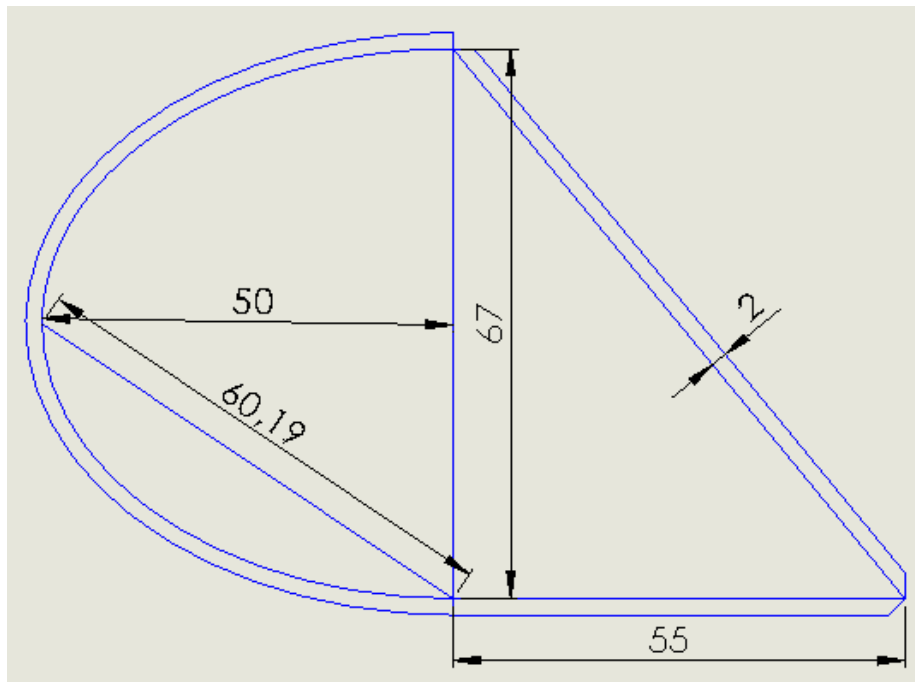
**Figure A-5** – Elliptical 140mm wings with stiffener and section measurements (mm), not to scale.





## Annex B – Tail designs

**Figure B-1** – Tail design with stiffener and section measurements (mm) (not to scale): Top- Vertical stabilizer and Rudder; Down- Horizontal stabilizer and Elevator.



## **Annex C – Wing Detailed Construction Process**

There are several steps to go through in order to successfully assemble a wing. Firstly, with the help of a ruler, a wing design has to be drawn on a A4 sheet. In the case of a 15% bigger than 140mm wing, a A3 sheet is needed. Once the wing is fully designed, a hard base has to be placed under it, and a mylar sheet on the top. At least four clamps have to be attached to the hard base, to make sure the mylar sticks to the paper sheet. Then, with a precision knife, the outer limit of the wing has to be cut. Be careful in order to keep mylar stretched, otherwise the wing measures will be incorrect. Once mylar wings are ready, stiffeners and wing rods can be measured and cut. The next stage is the glue process, in which carbon stiffeners are bonded onto mylar wings. Next, on a paper sheet, place a small quantity of glue. This has to be done every time a new stiffener is glued, once it becomes solid and loses its properties. The objective is to apply glue evenly on the stiffeners, however make sure it doesn't have too much, otherwise it will add excessive weight on the wings. It only has to have glue on the side that will be in contact with the wing. In order to move the stiffeners, use a pair of tweezers. This way, not only you avoid getting contaminated, but you will also have more precision when fixing the stiffeners on the wings. After all of them are attached, it is time to glue the wing rods. The process is the same, however, do not apply glue on the part that will fit in the flapping mechanism, which is about 1cm. Also, both the top and the base have to be glued, since mylar will be around them. Then, place the wing rods about 3mm under the top limit of the wing. This gap allows the mylar to stick around the wing rods. This step has to be done carefully, otherwise the wing shape will be affected. After sticking the leading edge, apply force with the fingers to prevent mylar from detaching.

After all the steps mentioned above are completed, the final stage takes place. In order to ensure that stiffeners don't come off due to the high frequency that wings are submitted, a reinforcement will be held. With a precision knife, cut small pieces of duct tape to glue the extremities of the stiffeners. They must be cut according to the shape of mylar, to guarantee the best fit. Every stiffener must

have two reinforcements: one at the bottom and another one at the top. Then, the hole that fixes the body clamp to the wing and the central part of the wing that attaches to the flapping mechanism, also have to be reinforced, preventing mylar from tearing up. With the help of the wing design sheet and the precision knife, cut a piece of duct tape in order to reinforce the wing center. The cut should be the same as the wing design, with a thickness no more than 5mm. So, place the wing design sheet over the duct tape, and cut right next to the paper. This ensures a proper fit to the wing center. In regard to the wing hole that connects to the body clamp, fix the wing to the flapping mechanism. Then, with a marker pen, draw a hole surrounding the body clamp. With a precision knife, cut the mylar excess and then reinforce the hole with duct tape. The easiest way is to cut and stick four equal parts of tape with a thickness no more than 5mm.

At least two hours are needed to complete the assembly of two wings. If possible, store them under pressure and wait one day before using them.

## **Annex D – Tail Detailed Construction Process**

The tail construction process is in every way similar to the wing assembly, since they are both made out of mylar and carbon rods. To begin, draw the tail design on a A4 sheet with the help of a ruler and compass. Then, place the sheet on a hard base and mylar over the tail design, securing it with at least four clamps. Make sure mylar is stretched to ensure measures are respected. With a precision knife, cut the outer limits of the tail design. After mylar is ready, cut 1mm carbon rods to the designed dimensions. Then, pour a drop of glue on a paper sheet and soak the carbon rods evenly, one at a time, adding glue every time a new rod is fitted. Place the rods on mylar with the help of a clamp, ensuring that they respect the 2mm gap from the outer limits. This gap enables mylar to be glued around the carbon rods. To ease up the carbon rod fixation on the rudder, secure it with a clamp when bending it. This is the most difficult step in the manufacturing process, once the rod has to be under pressure. After gluing and folding mylar around the rods, cut the bending zones that connect the rods between moving surfaces and stabilizers. This ensures an enhanced freedom, requiring less force to move the rudder and elevator.

After the assembly process is made, the tail can now be glued onto the main body. Place a thin layer of glue under the rear of the body rod and attach the horizontal stabilizer. After glue gets dry, reinforce the connection with duct tape. The same for the vertical stabilizer: apply glue on the rear of the body rod and fix the vertical stabilizer, reinforcing it by adding duct tape to the linkage.

## Annex E – Item Mass and source

**Table E-1** – Different FMWAV configuration, item mass and source

Item	Mass (grams)	URL
FWMAV (160; 150mAh)	19.3	-
FMWAV (140; 150mAh)	19.2	-
FWMAV (160; 120mAh)	17.8	-
FWMAV (140;120mAh)	17.7	-
150 mAh Batteries	6	<a href="http://shorturl.at/oAHKN">shorturl.at/oAHKN</a>
120 mAh Batteries	4.5	<a href="http://shorturl.at/gICJ0">shorturl.at/gICJ0</a>
On-board camera	3.6	<a href="http://shorturl.at/etUZ7">shorturl.at/etUZ7</a>
T-Tail	2.5	-
Flapping mechanism	2.18	-
160 high AR wing pair	1.5	-
140 wing pair	1.4	-
Brushless Motor	1.36	-
Magnetic Actuators	1.01	<a href="http://shorturl.at/ijtzG">shorturl.at/ijtzG</a> <a href="http://shorturl.at/inuKW">shorturl.at/inuKW</a>
DeiTang's Rx43d receiver	0.34	<a href="http://shorturl.at/fjwG5">shorturl.at/fjwG5</a>
Body rod	0.41	-
ESC	0.4	<a href="http://shorturl.at/amow6">shorturl.at/amow6</a>